NATIONAL ADVISORY COMMITTEE FOR AERONAUTICS

TECHNICAL NOTE 3115

ANALYSIS OF SWEPTBACK WINGS ON CAL-TECH ANALOG COMPUTER

By Richard H. MacNeal and Stanley U. Benscoter

California Institute of Technology

Washington

January 1954

V

NATIONAL ADVISORY COMMITTEE FOR AERONAUTICS

TECHNICAL NOTE 3115

ANALYSIS OF SWEPTBACK WINGS ON CAL-TECH ANALOG COMPUTER

By Richard H. MacNeal and Stanley U. Benscoter

SUMMARY

Using the Cal-Tech analog computer, structural analyses have been made of two 45° swept wings of aspect ratio 3. One of these has a constant depth and the other has a constant biconvex cross section in planes parallel to the air stream. The wings extend through the fuselage and are rigidly supported along two lines at the faces of the fuselage.

Deflections and all internal forces have been calculated for concentrated static loads. Vibration modes are also presented. The effects of neglecting shearing strains in the ribs and spars and also of assuming the ribs to be rigid have been investigated by modifying the electric circuits to correspond to these simplifications.

INTRODUCTION

Two 45° swept wings with aspect ratio 3 have been analyzed on the Cal-Tech analog computer for concentrated static loads which are symmetrical with respect to the airplane center line and are applied at points at the intersection of ribs and spars. Symmetrical vibration modes have also been calculated. One of these wings has a constant depth, while the other has a constant biconvex cross section in planes parallel to the air stream. The four wing spars have a 45° sweep in the swept portion of the wing and are unswept in the fuselage carry-through bay. The wing has simple rigid line supports at the faces of the fuselage.

The structural theory and analogous circuits for rectangular bays of multicell wings are given in references 1 and 2. Additional structural theory applicable to the swept leading- and trailing-edge spars is given in reference 3. Structural theory for the swept interior spars is developed in this paper.

The main purpose of this paper is to present the results of measurements made on the Cal-Tech computer. The diagrams present only a small portion of the data which were obtained from the computer, and which are given in complete form in the tables.

The effects of certain simplifications in the strucutral theory have been obtained by modifying the electrical circuits to correspond to these simplifications. The error due to neglecting the effect of shearing strains in the ribs and spars was investigated. The effect of assuming the ribs to be rigid was also determined.

This investigation was conducted at the California Institute of Technology under the sponsorship and with the financial assistance of the National Advisory Committee for Aeronautics.

SYMBOLS

A,B,C,D	sides of skin panel
A_{sm}	web area of spar s in bay m
a,b,c,d,e	displacements shown in figure 12
E	Young's modulus
F_{sm}	horizontal shear in mth bay of spar s
G	shearing modulus of elasticity
h	depth of wing
I_s	moment of inertia of spar
M_{ij}	bending moment in ith rib at jth spar
M_{ji}	bending moment in jth spar at ith rib
M_{si}	bending moment in spar s at ith rib
M_{sm}	bending moment in spar s at center of mth bay
ΔM_{sm}	moment load, hF_{sm}
N_{kp}	number of turns in primary winding of kth transformer
N_{ks}	number of turns in secondary winding of kth transformer
P_{ij}	concentrated load at intersection of ith rib and jth flange
Q	shearing force on skin panel

R	resistance
s	number of spar
T_{mn}	average chordwise twisting moment in cell mn
T_{nm}	average spanwise twisting moment in cell mn
$T_{mn}^{(+)}$	chordwise twisting moment at forward edge of cell mn
$T_{mn}^{(-)}$	chordwise twisting moment at rearward edge of cell mn
$T_{nm}^{(+)}$	spanwise twisting moment at outboard edge of cell mn
$T_{nm}^{(-)}$	spanwise twisting moment at inboard edge of cell mn
t	thickness of skin
t_k	kth transformer
V_{in}	shear in nth bay of ith rib
V_{sm}	shear in mth bay of spar s
w	deflection with shear strain in ribs and spars
w_{ij}	deflection at intersection of ith rib and jth flange
w_{si}	deflection at intersection of ith rib and spar s
β_{in}	rotation of normal in nth bay of ith rib
β_{jm}	rotation of normal in mth bay of jth spar
β_{sm}	rotation of normal in mth bay of spar s
$\gamma_{mn}^{(+)}$	shearing strain at forward edge of panel mn
$\gamma_{mn}^{(-)}$	shearing strain at rearward edge of panel mn
γ_{sm}	shearing strain in mth bay of spar s
Δ_i	jump in function across ith rib
θ_{sm}	slope of elastic curve in mth bay of spar s
λ	bay length or panel width

μ	Poisson's ratio
σ_x	spanwise normal stress
τ	shearing stress
τ_{xy}	shearing stress in covers parallel and perpendicular to the ribs

DESCRIPTION OF STRUCTURE

The two wings which have been analyzed have structural plan forms of aspect ratio 3. The first wing, which is shown in figure 1, has a rectangular cross section. The second wing, which is shown in figure 2, has a biconvex cross section of symmetrical parabolic shape. Each wing has a square fuselage bay with perpendicular ribs and spars. The outboard portion of each wing has a constant chord and a sweepback angle of 45°. The ribs are alined in a streamwise direction. The maximum thickness of the biconvex section is $7\frac{1}{2}$ percent of the theoretical aerodynamic chord measured in the streamwise direction.

No attempt has been made to determine the dimensions from design calculations. The dimensions are approximately the same as those which were used in reference 1 for the wing of aspect ratio 2. Since there is a smaller number of spars in the present case, the thickness of the webs of the spars has been increased somewhat. The number of spars which could be considered in the analysis was limited to four because of the available electrical equipment. Each spar in the wings which have been analyzed is equivalent to approximately three spars in the wing as it would be constructed.

The numbering system for the location of points on the plan form at which all quantities except twisting moments are measured is shown in figure 3. The points for twisting moments are indicated in figure 4. The numbers shown in figures 3 and 4 are used in recording the computed data in tabular form. The wings are assumed to be constructed of an aluminum alloy having the following physical properties:

$$E = 10.4 \times 10^6 \text{ psi}$$

$$G = 4.0 \times 10^6 \text{ psi}$$

$$\mu = 0.3$$

Specific weight = 0.107 lb/cu in.

Stiffness constants for the fuselage bay were computed in the manner described in reference 1 for straight wings. The structural theory and design of analogous circuits for the outboard region of the wing are given in the next section.

STRUCTURAL THEORY

The structural theory and corresponding analogous circuits for a straight multicell wing were derived in reference 2. These circuits may be used directly without change in the fuselage bay of the swept wings herein being treated. In reference 3 the structural theory and analogous circuit were derived for the leading edge of a delta wing. This circuit may be used in the present case for the leading- and trailing-edge regions outboard of the support. New structural theory and analogous circuits must be derived for the interior region of the wing outboard of the support.

The top and bottom skin material has been idealized by assuming that normal stresses are concentrated in stiffening elements which run parallel and perpendicular to the pane of symmetry of the aircraft. A layout of the idealized top skin is shown in figure 5. In the fuselage bay the stiffening elements serve as flanges for the ribs and spars. In the outboard portion of the wing the streamwise stiffening elements serve as flanges for the ribs. The spanwise stiffening elements will be referred to as flanges even though they are not connected to vertical shear webs. The orthogonal arrangement of flanges in the outboard region has been chosen in order to avoid the complications which arise in attempting to formulate internal force-displacement relations in skewed coordinates.

The cross-hatched panels represent idealized skin panels which are in a state of pure shear. In the region of the leading and trailing edges there are triangular panels which have been completely removed in forming the idealized structure. This skin material contributes to the flanges of the leading- and trailing-edge spars as explained in reference 3. The sweptback interior spars are shown by dotted lines to indicate that the spars in the idealized structure lie completely beneath the top skin. These interior spars are attached to the idealized skin panels at the center points only. The webs of these interior spars are connected to the webs of the ribs in such a manner as to obtain the same vertical deflection of the two members at the intersection point. The bending stiffness, as well as the shearing stiffness, of the interior spar is provided by the vertical web itself. The top skin of the wing is not considered to make any contribution to the bending stiffness of the interior spars.

A segment of interior spar s extending across the mth bay is shown in figure 6(a). This beam segment is acted upon by a concentrated moment load ΔM_{sm} at its center. This moment load is equal to the product of the force F_{sm} by the depth of the wing:

$$\Delta M_{sm} = hF_{sm} \tag{1}$$

The force F_{sm} is transmitted to an idealized panel of the top skin. The moment load causes a jump in the bending-moment diagram for the spar as shown in figure 6(b). The equation of moment equilibrium for the segment of spar is as follows:

$$M_{s(i+1)} - M_{si} - \Delta M_{sm} - V_{sm}\lambda\sqrt{2} = 0 \tag{2}$$

In designing the complete analogous circuit for the wing it is found that several transformers can be eliminated along the leading and trailing edges if the voltages in the moment circuits for the spars are assumed to be analogous to the product $\beta_{sm}\sqrt{2}$. This quantity is shown as the voltage at the upper nodal point in the circuit which is shown in figure 6(c). The layout of the circuit shown in figure 6(c) is the same as the beam circuit which is derived in detail in reference 4. It is necessary to consider the current which ordinarily represents bending moment to be analogous, in this case, to the quantity $M_{si}/\sqrt{2}$. This satisfies the requirement that the product of current by voltage drop across an element, which is a true electrical energy quantity, is also a true structural energy quantity. It may now be seen that equation (2) will become a statement of Kirchhoff's nodal law for the upper nodal point in figure 6(c) if it is divided through by $\sqrt{2}$ to obtain

$$\frac{M_{s(i+1)}}{\sqrt{2}} - \frac{M_{si}}{\sqrt{2}} - \frac{\Delta M_{sm}}{\sqrt{2}} - \lambda V_{sm} = 0 \tag{3}$$

If θ_{sm} is the slope of the elastic curve of the spar, it may be related to the deflections in finite difference form by the equation

$$\theta_{sm} = \frac{1}{\lambda\sqrt{2}}\left[w_{s(i+1)} - w_{si}\right] \tag{4a}$$

or

$$\theta_{sm}\sqrt{2} = (1/\lambda)\left[w_{s(i+1)} - w_{si}\right] \tag{4b}$$

An inspection of figure 6(c) shows that equation (4b) is a statement of the voltage relations for the transformer if the turns ratio is chosen as $1/\lambda$.

The slope of the elastic curve is also related to the rotation of the normal and the shearing strain in the shear web as follows:

$$\theta_{sm} = \beta_{sm} + \gamma_{sm} \tag{5}$$

The shearing strain may be expressed in terms of the section shear. Multiplying through equation (5) by $\sqrt{2}$ and rearranging the terms give

$$\theta_{sm}\sqrt{2} - \beta_{sm}\sqrt{2} = \left(\frac{\sqrt{2}}{\lambda G A_{sm}}\right)\left(\lambda V_{sm}\right) \tag{6}$$

It is evident that equation (6) expresses Ohm's law for the shear resistor if its resistance is assumed to be $\sqrt{2}/\lambda G A_{sm}$.

The moment resistor is determined by writing the relation between moment and curvature in finite difference form as follows:

$$\frac{1}{\lambda\sqrt{2}} \Delta_1 \beta_{sm} = -\frac{M_{si}}{EI_s} \tag{7}$$

Rearranging terms gives

$$\Delta_1\left(\beta_{sm}\sqrt{2}\right) = -\left(\frac{2\lambda\sqrt{2}}{EI_s}\right)\left(\frac{M_{si}}{\sqrt{2}}\right) \tag{8}$$

This equation expresses Ohm's law for the moment resistor and determines the magnitude of the resistance.

An idealized skin panel is shown in figure 7. The diagonal force F_{sm} is transmitted from the interior spar to the center point of the skin panel. It is assumed that only shearing forces act on the four sides of the panel. However, the forces Q_A, Q_B, Q_C, and Q_D are not equal in magnitude since they must have a resultant which is equal and opposite to F_{sm}. In order that the state of stress at the corners may be rational it would be necessary for the shearing stresses along the edges to vary in some manner such as is shown in the figure. However, the only value of stress that will be determined by the structural theory to be used is the average value on each side.

Since the panel is square, taking moments around the lower right-hand corner gives

$$Q_A = Q_B \tag{9}$$

Taking moments about the upper left-hand corner gives

$$Q_C = Q_D \tag{10}$$

Summing forces in the chordwise direction gives

$$Q_C - Q_A - \frac{F_{sm}}{\sqrt{2}} = 0 \tag{11}$$

Summing forces in the spanwise direction gives

$$Q_B - Q_D + \frac{F_{sm}}{\sqrt{2}} = 0 \tag{12}$$

If equations (9) to (12) are multiplied through by the depth of the wing the external shearing forces on the panel will be converted into twisting moments. The following definitions will be introduced:

$$-T_{nm}^{(-)} = hQ_A \tag{13a}$$

$$T_{mm}^{(+)} = hQ_B \tag{13b}$$

$$-T_{nm}^{(+)} = hQ_C \tag{13c}$$

$$T_{mm}^{(-)} = hQ_D \tag{13d}$$

In order to conform to the customary sign conventions of elastic plate theory it is necessary to associate negative spanwise twisting moment with positive shearing stress in the top skin. In formulating the structural theory in terms of first-order difference equations it would be more convenient to associate positive values of both spanwise and chordwise twisting moments with positive shearing stresses in the top skin.

After multiplying through equations (9) to (12) by h, equations (1) and (13) may be substituted to obtain the following:

$$-T_{nm}(-) = T_{mn}(+) \tag{14a}$$

$$-T_{nm}(+) = T_{mn}(-) \tag{14b}$$

$$-T_{nm}(+) + T_{nm}(-) - \frac{\Delta M_{sm}}{\sqrt{2}} = 0 \tag{15a}$$

$$T_{mn}(+) - T_{mn}(-) + \frac{\Delta M_{sm}}{\sqrt{2}} = 0 \tag{15b}$$

Equations (15) may be regarded as expressions of Kirchhoff's nodal law. Analogous nodal points are shown in figures 8(a) and 8(b). These nodal points both correspond to the physical center point of the idealized panel shown in figure 7. The wires which carry the current $\Delta M_{sm}/\sqrt{2}$ must be connected to the upper nodal point of the spar circuit shown in figure 6(c). A transformer t_2 is required for this purpose. This transformer, which is shown in figures 8(c) and 8(d), has a one-to-one turns ratio. The connected circuits are shown in figures 8(e) and 8(f). These circuits are consistent with the spar circuit of figure 6(c).

The complete circuits carrying currents that are analogous to twisting moments may now be designed. In order to begin the design the circuit elements for a standard panel of a straight wing may be taken from reference 2 and redrawn in a modified form as shown in figures 9(a) and 9(b). In figure 9(a) the current representing spanwise twisting moment passes through the secondary winding of transformer t_1. This winding is indicated as being divided into two equal parts with a center tap. The current representing chordwise twisting moment is shown in figure 9(b) where the primary winding of transformer t_1 also has a center tap. The resistance which is in series with the primary winding has been divided into two equal parts.

It is now necessary to recognize that the center taps of transformer t_1 are the nodal points of figure 8. If the nodal points of figures 8(e) and 8(f) are superposed on the center taps of the transformer in figures 9(a) and 9(b) the resulting circuit will appear as shown in figures 9(c) and 9(d). When current enters a transformer winding at an intermediate tapped position, each segment of the winding will carry a different current. In such a case the law of currents for the transformer requires that the sum of products of current by number of turns for each segment of the primary winding shall equal the corresponding sum for the segments of the secondary winding. The present case is greatly simplified by the fact that the half windings of the

primary and secondary coils have the same number of turns and the current entering the center tap of the secondary winding is equal to the current leaving the primary winding. This latter condition is guaranteed to be true by the current law for the transformer t_2. Because of these simplifications the current law for t_1 may be reduced to equation 14(a) or 14(b). Thus the twisting-moment circuit satisfies all equilibrium conditions.

The remaining feature of the designing of the twisting-moment circuit consists of determining the size of the resistors. For this purpose the circuit of figure 9(d) has been enlarged and drawn as figure 10 where the voltages at all of the nodes are given. In order to determine the size of the resistors it is necessary to write Ohm's law for the resistors. An analogous structural equation must then be derived from an application of Hooke's law to the idealized skin panel.

In order to write Ohm's law for the resistors it is necessary to determine the voltages at the interior nodal points. Since t_1 has a one-to-one turns ratio the voltage drop across the primary coil must equal the known drop across the secondary coil. Because of the voltage law for transformers the voltage at the center tap of the secondary coil of t_1 (see fig. 9(c)) must equal the average of the known values at the ends of the winding. This voltage, $(1/2)\left[\beta_{in} + \beta_{(i+1)n}\right]$, becomes immediately the voltage drop across the secondary of t_2 and hence is also the voltage drop across the primary of t_2. This gives immediately the formula for the voltage at the center tap of the primary of t_1 as shown in figure 10. Since the voltage drop across each half winding must equal one-half of the drop across the total winding the voltage at each end of the primary of t_1 may be determined to be as shown in figure 10. Ohm's law for the resistors may now be written as follows:

$$R_1 T_{mn}^{(+)} = \beta_{sm}\sqrt{2} + \beta_{in} - \beta_{(j+1)m} \tag{16a}$$

$$R_2 T_{mn}^{(-)} = \beta_{jm} - \beta_{sm}\sqrt{2} - \beta_{(i+1)n} \tag{16b}$$

It is now necessary to develop equations relating internal forces to displacements. These equations must take the same form as equations (16) and yield formulas for R_1 and R_2. In figure 11(a) the idealized panel is shown with the forces which act on it. Dotted lines indicate the sections along which the panel is cut to form three pieces as shown in figure 11(b). Because of the relations given by equations (9) and (10) it can be shown from statics that there are no shearing forces on the cut sections. The normal stresses are assumed to be uniformly distributed.

If the external shearing forces are also assumed to be uniformly distributed each triangular panel is in a uniform state of pure shear. These assumptions regarding stress distributions are obviously one of the sources of error in the method of analysis. The narrow diagonal strip on which F_{sm} acts must be considered to have a negligible width.

In order to establish force-displacement relations it is necessary to introduce a definition of shearing strain in each of the triangular panels. For this purpose the two triangular panels are shown in figure 12. In figure 12(a) points A, B, and E are the midpoints of the sides. Shearing strain is defined as the increase in angle AEB which takes place under load. Similarly in the outboard triangle shown in figure 12(b) the shearing strain is defined as the increase which occurs under load in angle CED. It may be seen that a displacement of points A, B, C, or D normal to their edges will cause no shearing strain. Also it may be noted that a motion of point E in a direction parallel to the diagonal edge causes no shearing strain. For convenience the distorted panels have been drawn with only a normal component of displacement at point E.

At points A, B, C, D, and E the components of displacements which contribute to the shearing strains are indicated as a, b, c, d, and e. The shearing strain in the inboard triangle will be indicated as $\gamma_{mn}^{(+)}$ while the shearing strain in the outboard triangle will be indicated by $\gamma_{mn}^{(-)}$. These strains may be expressed in terms of the displacements as follows:

$$\gamma_{mn}^{(+)} = (2/\lambda)\left(\frac{e}{\sqrt{2}} - a + \frac{e}{\sqrt{2}} - b\right) \tag{17a}$$

$$\gamma_{mn}^{(-)} = (2/\lambda)\left(c - \frac{e}{\sqrt{2}} + d - \frac{e}{\sqrt{2}}\right) \tag{17b}$$

The displacements can be expressed in terms of the rotations of the normals by the following formulas:

$$a = -(h/2)\beta_{in} \tag{18a}$$

$$b = (h/2)\beta_{(j+1)m} \tag{18b}$$

$$c = -(h/2)\beta_{(i+1)n} \tag{18c}$$

$$d = (h/2)\beta_{jm} \tag{18d}$$

$$e = (h/2)\beta_{sm} \tag{18e}$$

Substituting equations (18) into equations (17) gives:

$$\gamma_{mn}^{(+)} = (h/\lambda)\left[\beta_{in} - \beta_{(j+1)m} + \beta_{sm}\sqrt{2}\right] \tag{19a}$$

$$\gamma_{mn}^{(-)} = (h/\lambda)\left[\beta_{jm} - \beta_{(i+1)n} - \beta_{sm}\sqrt{2}\right] \tag{19b}$$

The shearing strains are related to the twisting moments by the formulas

$$\gamma_{mn}^{(+)} = \frac{T_{mn}^{(+)}}{\lambda thG} \tag{20a}$$

$$\gamma_{mn}^{(-)} = \frac{T_{mn}^{(-)}}{\lambda thG} \tag{20b}$$

Substituting equations (20) into equations (19) and introducing I as the moment of inertia of the skin per unit of length give

$$\left(\frac{1}{2GI}\right) T_{mn}^{(+)} = \beta_{in} - \beta_{(j+1)m} + \beta_{sm}\sqrt{2} \tag{21a}$$

$$\left(\frac{1}{2GI}\right) T_{mn}^{(-)} = \beta_{jm} - \beta_{(i+1)n} - \beta_{sm}\sqrt{2} \tag{21b}$$

It is now seen that equations (21) have the same form as equations (16) and that the resistances are given by

$$R_1 = R_2 = \frac{1}{2GI} \tag{22}$$

The sum of the two resistances R_1 and R_2 is equal to the resistance which would be used if there were no diagonal spar beneath the skin panel.

The design of the circuit elements carrying currents that are analogous to bending moments is the same as for a straight wing. The design of the circuit for the leading- and trailing-edge members is the same as that which was used for the leading edge of the delta wing in reference 3.

The limitations upon direct applicability of the theory herein presented should be noted. From the above structural theory it can be seen that the interior spars must lie along true diagonals of the idealized

skin panels. This means that the idealized spars and ribs must be equally spaced. The actual ribs and spars of a given wing must be replaced by equivalent ribs and spars in the idealized structure. The spacing of the idealized spars may be considered to be arbitrary and will depend upon the amount of electrical equipment which is available. The spacing of the ribs is determined by the spacing of the spars and the sweep angle. For sweep angles other than 45° the idealized skin panels become rectangular. For very large or very small sweep angles the rib spacing becomes impracticable. The method of analysis cannot be applied directly to swept wings with variable chord.

LOADING CONDITIONS

The plan forms of the wings are symmetrical about the plane of symmetry of the aircraft. Only symmetrical loading conditions have been used since the antisymmetric conditions would require more electrical equipment than is available at present on the Cal-Tech analog computer. The loads have been applied to the wing in symmetrical pairs of concentrated forces. For each position of the concentrated force, deflections, shears, bending moments, and twisting moments were measured at all points. Loads were applied at the intersection points of ribs and spars as shown in figure 3. When measuring deflections all points were loaded one at a time. When measuring internal forces only points outboard of the support were loaded. The boundary conditions, symmetry conditions, and support conditions are the same as for the straight and delta wings and are discussed in detail in references 1 and 3.

A few special cases were computed in order to provide data that might be useful in future efforts to formulate more elementary structural theories. For the wing with rectangular cross section analyses were made for the case of the ribs being infinitely stiff in bending but with finite shearing stiffness. A second case was computed with the ribs infinitely stiff in bending and shear. A third case was computed in which the effect of shearing strains in both the ribs and spars was omitted. For these three cases the wing was loaded at points 91 and 97. For the wing with biconvex section a special case was computed in which the shear web of the rear spar was cut just outboard of the support. This was done by removing the corresponding resistor from the circuit. For this case the wing was loaded at point 91.

TREATMENT OF DATA FROM COMPUTING MACHINE

The computed results are contained in tables 1 to 5. In the process of converting electrical measurements to structural quantities correction factors were introduced to satisfy the static conditions for the total

bending moment over the support and the total shear in the first bay outboard of the support. This correction factor as well as the sources of error involved in the use of the analog computer is discussed in detail in reference 1.

The deflections which are given in the tables are in inches for a concentrated load of 1 kip on each half of the wing. The internal forces correspond to a concentrated load of 1 pound on each half of the wing. The internal forces which are given in the tables are the total forces in an element of the idealized wing rather than the force per unit of width as is used in elastic plate theory. The twisting moments which are recorded in the tables are computed as the average values of $T_{nm}^{(-)}$ and $T_{nm}^{(+)}$ as defined in the structural theory.

ELECTRIC CIRCUITS

The complete electric circuit is shown in three parts in figures 13, 14, and 15. In figure 13 there is a planar circuit in which the currents represent shears in the ribs and spars and the voltages represent deflections. In addition there are linear circuits along the outboard spars in which the currents represent bending moments in the idealized spars. The condition of symmetry requires that there shall be no spanwise shears at the plane of symmetry of the aircraft. Hence no circuit elements appear across the plane of symmetry. The nodal points along the support are grounded since the deflections must be zero along this line. The bending moments along the leading edge and the trailing edge in the spars are computed at the center of the bays rather than at intersection points of ribs and spars.

In figure 14 the currents represent spanwise bending moments and chordwise twisting moments in the idealized skin material. In the fuselage bay the circuit is the same as for a straight wing. In the outboard region the bending resistors are designed in the same manner as for a straight wing. The currents representing twisting moments are carried in elements which are designed according to the structural theory herein contained. At the plane of symmetry of the aircraft the spanwise rotations of normals in the spars must be zero. Hence these voltages are grounded.

In figure 15 the currents represent chordwise bending moments and spanwise twisting moments. The bending-moment elements are designed as in a straight wing. The twisting-moment elements are designed according to the theory herein contained. At the plane of symmetry the spanwise twisting moments must be zero. Hence no corresponding circuit elements appear at the plane of symmetry. Along the support it has been assumed

that the chordwise rotation of the normals will be restrained to be zero by the supporting structure. Hence these nodal points are grounded.

A few comments concerning the choice of scale factors which were used in designing the electric circuits may be of interest. The structural quantities which correspond to resistances or turns ratios of the transformers must be multiplied by appropriate scale factors to determine the actual circuit elements. The measured currents and voltages, as obtained from the meter, must be multiplied by appropriate scale factors to determine the true values of the corresponding structural quantities. After the scale factors have been chosen for designing the circuit elements the scale factors for the computed quantities are obtained from the basic equations of the structural theory. A theoretical discussion of scale factors is given in the appendix to reference 5.

From a proper choice of scale factors relating displacements and voltages it was possible to make all of the transformer turns ratios equal to unity. The remaining scale factors were chosen to require resistors ranging from 50 to 5,000 ohms with currents not exceeding 30 milliamperes. The maximum voltage did not exceed 50 volts. The frequency of operation, chosen to give minimum error from parasitic effects, was 100 cycles per second.

PRESENTATION OF RESULTS

The data taken from the analog computer are presented by means of tables and diagrams. All of the data are given in tables 1 to 5. Deflections, shears, spanwise and chordwise bending moments in the idealized orthogonal flanges, bending moments in the idealized diagonal spar flanges, and the values of twisting moments at the center of each square shear panel are given for each loading condition. Some of the data have been presented in diagrams. The data so presented have been chosen to illustrate points of interest, particularly the effects of simplifications in the structural theory.

The internal forces for six loading conditions are given in planform diagrams in figures 16 to 24. These diagrams are of three kinds: One kind shows the distribution of shears in the ribs and spars (figs. 16 to 18); the second kind shows the distribution of spanwise bending moments, chordwise twisting moments, and the bending moments in the leading- and trailing-edge spars (figs. 19 to 21); the third kind shows chordwise bending moments and spanwise twisting moments (figs. 22 to 24). These diagrams should give the reader a good idea of the distribution and interdependence of the internal forces. The arrows show the paths along which the forces are transmitted. In the shear-distribution diagrams,

the inflow at each junction should equal the outflow. In the other two types of diagram, inflow and outflow will not balance because the increments in moments due to rib and spar shears and the moments in the internal diagonal spar flanges are not shown in the diagrams.

Chordwise distributions of deflections and internal forces as well as vibration modes and other miscellaneous curves are given in figures 25 to 36.

DEFLECTIONS

Chordwise-deflection curves for the wing of biconvex section are compared in figure 25 for loads applied at points 91 and 97. Because of its eccentricity the load at point 91 causes considerably larger deflections along the trailing edge than the load at point 97. The rotations of the chordwise cross sections are nearly zero for a load at point 97.

In figure 26 a load is applied to point 91 of the wing with rectangular cross section and the resulting deflections for the case of elastic ribs are compared with the deflections for the case of rigid ribs. In the case of rigid ribs the average deflection of any cross section agrees well with the average deflection in the elastic-rib case, but the angle of twist of the cross sections appears to differ considerably. A similar comparison is made in figure 27 for a load at point 97, where the agreement appears to be better. In figure 28 deflections are compared for the same wings for an upload at point 91 and a download at point 97. In this case the rotation of the chordwise cross section at the tip in the case of rigid ribs is only 57 percent of the rotation observed with elastic ribs. It should be remembered that in the cases with rigid ribs the shearing flexibility of the spars has been retained.

The effect of shearing strain in the ribs and spars on deflections is illustrated in figure 29 for the wing of rectangular cross section. For a load at point 91, the effect of shearing strains is to increase deflections along the trailing edge by about 9 percent. The increase in deflections along the leading edge is much smaller and near the support a small decrease is observed. For a load applied at point 97 the effect is reversed. Consequently if a torque is applied to the tip, the rotation of the chordwise cross section at the tip is decreased by about 20 percent when shearing strains in the ribs and spars are omitted.

SHEARS

The distribution of shears is illustrated in plan-form diagrams in figures 16 to 18. As in the case of the delta wing (ref. 3) the shear in the ribs tends to flow toward the leading edge in the tip rib and toward the trailing edge in the ribs farther inboard, for all loading conditions. This behavior helps to distribute the spanwise bending moment more evenly.

In figure 16, which compares shear distribution in the wings of rectangular and biconvex sections for a load at point 73, it is seen that the shape of the cross section does not have a large effect on the shear distribution.

The effect of the omission of shearing strain in the ribs and spars is illustrated in figure 17 for a load at point 91. The shear in the rear spar is increased 25 percent near the support when shear strains are omitted.

It will also be observed in this figure that the shear flow in the leading edge near the support is negative, as a result of the large eccentricity of the load.

The effect of making the ribs rigid is illustrated in figure 18 for a load at point 97. The discrepancy in this case is as much as 50 percent.

SPANWISE BENDING MOMENTS AND BENDING MOMENTS IN SPARS

The term "spanwise bending moments" as used in this paper refers to the bending moments in the flanges of the idealized structure oriented normal to the ribs (see fig. 5). The term "bending moments in the spars" refers to the bending moments carried by the idealized spars which are parallel to the leading edge.

The distribution of spanwise bending moments and of the bending moments in the spars is shown in plan-form diagrams in figures 19 to 21 along with the chordwise twisting moments. The small bending moments carried by the two interior spars in the portion of the wing outboard of the support are not shown in these diagrams.

In figures 30 to 32, spanwise normal stresses at points just to the left of the support are shown. In figure 30 it is shown that, for the wing with biconvex cross section loaded anywhere along ribs 7 or 9, the maximum spanwise normal stress over the support occurs between spars 1 and 3. The chordwise location of the load has only a small effect on the

magnitude and location of the maximum stress. In figure 31 spanwise normal stresses along the support for a load at point 91 on the wing of rectangular cross section are shown. In this case a considerable stress concentration exists at the rear spar. It appears that the assumption of rigid ribs and the assumption of no shearing strains in the ribs and spars give good results in this case.

A similar comparison is made in figure 32 for a load at point 97. In this case the maximum stress also occurs at the trailing edge, although its magnitude is considerably less than for a load at point 91.

A discussion of the general effects of the assumptions of rigid ribs and of infinite shearing stiffness in the spars is given in reference 3.

TWISTING MOMENTS

The distribution of chordwise twisting moments is shown in plan-form diagrams in figures 19 to 21. These are numerically equal to the spanwise twisting moments which are shown in similar diagrams in figures 22 to 24.

The chordwise distribution of spanwise shearing stresses in the skin at points midway between ribs 3 and 5 is shown in figure 33 for the wing of rectangular cross section. At the leading and trailing edges the spanwise shearing stress was computed from the bending moment in the spar flanges of the idealized structure. This is permissible because there are no normal stresses perpendicular to the free edges. At the two interior points shearing stresses were computed from the average twisting moments in the rectangular shear panels of the idealized structure.

In figure 33(a) the distribution of shearing stress is shown for a load at point 91. In the wing with elastic ribs the shearing stress is much greater at the trailing edge than at the leading edge. When shearing strains in the ribs and spars are omitted, the shearing stress is uniformly decreased by a small amount. In the case of rigid ribs the chordwise variation of shearing stress is much less pronounced. Similar observations can be made from figure 33(b), for which the load is at point 97.

CHORDWISE BENDING MOMENTS

The bending moments in the ribs are illustrated in plan-form diagrams in figures 22 to 24. For the case of rigid ribs, the bending moments shown are in equilibrium with twisting moments and rib shears. They are not equal to Poisson's ratio times the spanwise bending moments. The

bending moments in the ribs are compared in figure 34 for the cases of elastic ribs and ribs which are rigid in bending but elastic in shear. The bending moment in the tip rib shows fairly good agreement between the elastic and rigid cases for either a load at point 91 or a load at point 97. In rib 5, the rigid-rib case shows roughly 25 percent greater maximum bending moment than the elastic case.

For a load at point 91 the rib bending moments are as large as the spanwise bending moments because of the eccentricity of the load.

VIBRATION MODES

Vibration modes were measured in the same way for the 45° swept wing as they were for the delta wing and the wing of rectangular plan form so that the remarks in reference 1 concerning vibration modes apply to the 45° swept wing. Symmetric vibration modes were measured for both the wing of rectangular cross section and the wing of biconvex cross section. Frequencies and deflections are recorded in tables 4 and 5. Symmetric modes for the wing of rectangular cross section are illustrated in figure 35 by means of contour drawings.

The first mode at 36.0 cycles per second may be described as the first bending mode and shows lines of equal deflection perpendicular to the swept edges. The second mode at 114 cycles per second may be described as the first torsion mode and shows a line of zero-deflection intersecting the line of support at the trailing edge. The third and fourth modes, which are only 10 percent apart in frequency, seem to combine a second bending mode of the outboard wing with large bending amplitudes of the fuselage carry-through bay.

The difficulties that would be involved in replacing the 45° swept wing by an equivalent beam for dynamic analyses are made evident by the contour lines.

CONCLUSIONS

The foregoing discussion of the results of an analysis of a swept-back wing on the Cal-Tech analog computer is based upon the data presented in the figures which include only a small portion of all the data taken. The reader will find that the data in the tables will permit him to make a more thorough study of any particular case in which he may be interested. For example he can combine the results for several concentrated loads to find the results for a particular distributed load. The problems analyzed in this paper utilized the Cal-Tech analog computer for 2 weeks. The results and conclusions of the investigation are as follows:

1. For the wing of rectangular cross section very high spanwise normal stresses were found to exist at the intersection of the trailing edge with the face of the fuselage for loads applied along the tip. The magnitude of the maximum stress was considerably reduced and its location was shifted slightly forward in the case of the biconvex wing.

2. For the wings analyzed in this paper, which have homogeneous skin coverings without heavy concentrated flanges, it has been found that the shearing stresses in the skin and the chordwise normal stresses are of the same order of magnitude as the spanwise normal stresses for loads applied at the tip, particularly for loads applied at the rear corner. For the delta wing analyzed in NACA TN 3114, these stresses were found to be small for a concentrated load located anywhere on the plan form.

3. The effects of neglecting shearing strains in the ribs and spars and also of assuming the ribs to be rigid have been investigated by modifying the electric circuits to correspond to these simplifications. It has been found that the omission of shearing strains produces errors in the deflections of the order of 10 percent or less. The assumption of rigid ribs gives good results for the average deflection of any rib and for the distribution of spanwise normal stress; it produces errors of the order of 25 percent in the distribution of spanwise twisting moments, rib bending moments, and the shears in the ribs and spars; it gives surprisingly poor results for torsional deflections due to a couple applied to the tip. It should be emphasized that the conclusions concerning the effects of these assumptions cannot be applied to an analysis in which both the assumption of rigid ribs and the assumption of no shearing strains in the spars are made simultaneously.

4. The results of this paper indicate that, for wings of low aspect ratio, the elastic camber of the ribs has a significant influence upon the deflections and internal stress distributions.

California Institute of Technology,
Pasadena, Calif., March 24, 1953.

REFERENCES

1. Benscoter, S. U., and MacNeal, R. H.: Analysis of Straight Multicell Wings on Cal-Tech Analog Computer. NACA TN 3113, 1953.

2. Benscoter, S. U., and MacNeal, R. H.: Equivalent Plate Theory for A Straight Multicell Wing. NACA TN 2786, 1952.

3. MacNeal, R. H., and Benscoter, S. U.: Analysis of Multicell Delta Wings on Cal-Tech Analog Computer. NACA TN 3114, 1953.

4. Benscoter, S. U., and MacNeal, R. H.: Introduction to Electrical-Circuit Analogies for Beam Analysis. NACA TN 2785, 1952.

5. MacNeal, R. H., McCann, G. D., and Wilts, C. H.: The Solution of Aeroelastic Problems by Means of Electrical Analogies. Jour. Aero. Sci., vol. 18, no. 12, Dec. 1951, pp. 777-789.

TABLE 1

WING WITH RECTANGULAR SECTION

(a) Deflections

Deflection point	Deflection, in./kip, at loading point -															
	11	13	15	17	51	53	55	57	71	73	75	77	91	93	95	97
11	0.0216	0.0096	0.0050	0.0037	-0.0100	-0.0085	-0.0074	-0.0063	-0.0194	-0.0180	-0.0164	-0.0150	-0.0294	-0.0279	-0.0264	-0.0248
13		.0119	.0064	.0050	-.0069	-.0067	-.0063	-.0058	-.0138	-.0136	-.0132	-.0128	-.0213	-.0210	-.0207	-.0200
15			.0119	.0096	-.0053	-.0057	-.0062	-.0065	-.0106	-.0110	-.0116	-.0122	-.0159	-.0165	-.0171	-.0175
17				.0222	-.0047	-.0057	-.0068	-.0084	-.0094	-.0106	-.0118	-.0132	-.0141	-.0153	-.0165	-.0177
51					.0423	.0242	.0152	.0095	.0768	.0582	.0425	.0298	.1101	.0926	.0744	.0580
53						.0266	.0179	.0126	.0474	.0438	.0384	.0324	.0694	.0647	.0598	.0538
55							.0238	.0166	.0302	.0322	.0344	.0341	.0442	.0457	.0472	.0483
57								.0228	.0186	.0224	.0269	.0326	.0272	.0313	.0354	.0400
71									.1890	.1331	.0941	.0640	.2893	.2336	.1800	.1348
73										.1158	.0903	.0678	.2064	.1835	.1556	.1289
75											.0896	.0726	.1438	.1376	.1334	.1235
77												.0802	.0968	.1021	.1067	.1134
91													.5190	.3874	.2902	.2148
93														.3396	.2686	.2112
95															.2532	.2086
97																.2127

TABLE 1.- Continued

WING WITH RECTANGULAR SECTION

(b) Spanwise shears

Shear point	Spanwise shear, lb/lb, at loading point -											
	51	53	55	57	71	73	75	77	91	93	95	97
21	-0.059	-0.016	0.003	0.015	-0.092	-0.056	-0.018	0.007	-0.130	-0.095	-0.061	-0.024
23	-.003	-.022	-.001	.008	-.035	-.039	-.042	-.023	-.068	-.067	-.070	-.071
25	.019	.002	-.024	.004	.033	.014	-.009	-.031	.050	.032	.013	-.009
27	.041	.035	.022	-.028	.092	.080	.069	.047	.145	.130	.117	.103
41	.793	.352	.114	0	.784	.522	.274	.069	.834	.589	.368	.158
43	.190	.426	.268	.132	.284	.311	.300	.259	.327	.326	.312	.297
45	.049	.155	.425	.279	.045	.143	.266	.331	.028	.125	.221	.304
47	-.032	.067	.193	.588	-.113	.024	.160	.340	-.190	-.040	.099	.241
61	-.122	.038	.011	-.013	.615	.263	.082	-.007	.498	.318	.162	.045
63	.030	-.118	.035	.024	.237	.405	.246	.116	.339	.326	.270	.201
65	.069	-.003	-.115	.075	.167	.203	.404	.276	.211	.245	.309	.305
67	.011	.075	.062	-.091	-.011	.125	.264	.614	-.040	.109	.254	.445
81	-.007	-.002	-.004	-.003	-.126	-.003	-.010	-.012	.530	.122	.011	-.006
83	-.024	-.019	-.002	-.003	-.052	-.127	.015	.004	.183	.489	.212	.083
85	-.008	-.014	-.015	.004	.062	-.006	-.111	.047	.169	.181	.499	.222
87	.026	.025	.013	-.004	.082	.112	.086	-.059	.139	.202	.269	.690

TABLE 1.- Continued

WING WITH RECTANGULAR SECTION

(c) Chordwise shears

Shear point	Chordwise shear, lb/lb, at loading point -											
	51	53	55	57	71	73	75	77	91	93	95	97
12	0.059	0.015	-0.003	-0.015	0.091	0.055	0.018	-0.007	0.128	0.094	0.059	0.023
14	.061	.037	-.001	-.023	.127	.095	.061	.016	.196	.162	.131	.094
16	.042	.035	.023	-.027	.093	.081	.069	.047	.145	.130	.118	.103
52	-.098	.312	.104	.014	.182	.262	.192	.075	.343	.276	.205	.113
54	.064	-.152	.336	.122	.224	.160	.247	.218	.328	.274	.246	.206
56	.041	.007	-.131	.327	.099	.100	.106	.273	.143	.150	.156	.203
72	-.116	.041	.014	-.011	-.308	.266	.092	.003	-.023	.194	.151	.049
74	-.061	-.059	.050	.016	-.015	-.225	.323	.115	.139	.037	.208	.164
76	.017	-.049	-.050	.086	.090	-.013	-.181	.341	.179	.091	.013	.247
92	-.005	0	-.003	-.002	-.119	.002	-.007	-.008	-.532	.132	.018	0
94	-.025	-.018	-.003	-.004	-.162	-.120	.012	-.001	-.329	-.408	.240	.089
96	-.030	-.029	-.016	.002	-.090	-.121	-.095	.049	-.153	-.216	-.285	.323

TABLE 1.- Continued

WING WITH RECTANGULAR SECTION

(d) Spanwise bending moments

Moment point	Spanwise bending moment, in-lb/lb, at loading point -											
	51	53	55	57	71	73	75	77	91	93	95	97
11	-4.21	-3.46	-2.92	-2.46	-8.16	-7.46	-6.58	-5.90	-12.21	-11.46	-10.74	-9.96
13	-5.80	-5.69	-5.19	-4.75	-11.74	-11.54	-11.28	-10.70	-17.82	-17.52	-17.19	-16.86
15	-4.25	-4.70	-5.25	-5.31	-8.62	-9.12	-9.72	-10.30	-12.87	-13.35	-13.83	-14.43
17	-1.72	-2.13	-2.63	-3.47	-3.36	-3.90	-4.42	-5.08	-5.07	-5.58	-6.06	-6.63
$31^{(-)}$	-6.83	-4.72	-3.53	-2.56	-12.60	-10.76	-8.76	-7.12	-18.66	-16.86	-15.03	-12.96
33	-5.00	-5.48	-4.56	-4.01	-11.02	-10.98	-10.86	-9.98	-16.98	-16.86	-16.77	-16.59
35	-3.38	-4.18	-5.30	-4.43	-7.00	-7.86	-8.88	-9.98	-10.44	-11.31	-12.12	-13.17
37	-.80	-1.61	-2.60	-5.00	-1.38	-2.40	-3.48	-4.94	-1.92	-3.00	-4.05	-5.28
$31^{(+)}$	1.99	-.94	-2.21	-2.51	-.06	-2.60	-4.12	-5.44	-2.76	-4.92	-7.05	-8.49
51	2.43	2.18	.52	-.26	6.32	2.54	.54	-.74	6.99	3.18	.84	-.96
53	-.67	.18	-.27	-.99	-6.20	-6.10	-5.14	-4.68	-12.42	-12.15	-11.82	-10.62
55	-1.67	-.86	-.12	-.44	-5.86	-6.04	-6.54	-5.62	-10.50	-10.83	-11.49	-12.33
57	.13	-.47	-.60	-2.94	.14	-1.20	-2.62	-5.36	0	-1.56	-3.06	-5.13
71	-.27	.41	.13	-.04	1.88	1.98	.48	-.14	6.81	1.38	-.09	-.42
73	1.57	.33	.33	.10	1.88	1.82	.98	-.20	-2.58	-3.72	-2.85	-2.31
75	-.47	-.25	-.40	0	-2.38	-1.50	-.74	-.74	-6.12	-6.54	-7.95	-6.84
77	.39	-.56	-.93	-.15	.92	-.58	-1.32	-3.96	1.02	-.93	-2.91	-7.14
97	.26	-.08	-.22	.10	1.08	-.02	-.78	-.22	2.55	1.17	.15	-4.83

TABLE 1.- Continued

WING WITH RECTANGULAR SECTION

(e) Chordwise bending moments

Moment point	Chordwise bending moment, in-lb/lb, at loading point -											
	51	53	55	57	71	73	75	77	91	93	95	97
13	-0.70	-0.77	-0.70	-0.57	-1.50	-1.50	-1.52	-1.44	-2.34	-2.34	-2.34	-2.31
15	-.49	-.62	-.72	-.66	-1.04	-1.16	-1.30	-1.40	-1.59	-1.71	-1.83	-1.98
51	-2.40	-2.17	-.52	.26	-6.20	-2.48	-.52	.74	-6.81	-3.06	-.81	.99
53	-5.08	3.03	.38	.42	-11.00	-5.16	-.72	.70	-15.60	-10.26	-5.13	-1.47
55	-3.42	-.81	4.75	.58	-7.78	-4.46	-.90	1.78	-11.82	-8.25	-4.74	-1.23
57	-.17	.46	.60	2.95	-.16	1.20	2.60	5.36	-.06	1.50	3.03	5.16
71	.32	-.40	-.13	.04	-1.80	-1.94	-.46	.14	-6.63	-1.32	.18	.45
73	-.90	.21	0	-.05	-7.38	2.50	.36	.28	-15.66	-6.84	-.42	.42
75	-1.68	.95	.83	-.27	-6.56	-1.82	5.22	1.08	-12.30	-6.96	-1.26	2.46
77	-.39	.55	.94	.17	-.90	.48	1.32	3.98	-1.11	.84	2.88	7.14
93	-.04	.01	-.04	-.03	-1.80	.08	-.10	-.12	-8.28	2.19	.33	.03
95	-.70	.15	.05	-.14	-2.44	.16	.60	-.28	-6.78	-2.94	4.17	1.08
97	-.27	.08	.23	-.09	-1.10	0	.80	.26	-2.58	-1.20	-.12	4.89

TABLE 1.- Continued

WING WITH RECTANGULAR SECTION

(f) Bending moments in spars

Moment point	Bending moments in spar, in-lb/lb, at loading point -											
	51	53	55	57	71	73	75	77	91	93	95	97
41	-3.28	-1.29	-0.55	-0.08	-8.76	-5.62	-3.36	-1.64	-13.23	-10.26	-7.26	-4.68
61	1.22	.18	.14	.14	-1.48	-.14	0	.14	-7.80	-4.23	-2.16	-.93
81	.10	.04	.06	.04	1.52	.12	.16	.14	-5.67	-1.20	0	.12
53	-.18	.10	.04	.04	-.64	-.46	-.20	-.06	-1.11	-.84	-.60	-.33
73	.01	-.04	0	.01	-.22	.06	.02	.02	-.78	-.60	-.21	-.09
55	-.20	-.06	.17	.08	-.56	-.42	-.32	-.08	-.93	-.75	-.63	-.42
75	-.07	0	-.03	.03	-.34	-.14	.12	.08	-.75	-.54	-.48	-.12
47	-1.51	-1.48	-1.47	-.38	-3.20	-3.14	-3.16	-3.20	-4.80	-4.71	-4.68	-4.68
67	-1.56	-.51	.62	1.20	-4.30	-3.14	-1.96	.20	-7.38	-6.15	-5.01	-3.99
87	-.62	-.16	.18	-.10	-2.32	-1.16	.20	.98	-4.86	-3.81	-3.15	-1.05

TABLE 1.- Concluded

WING WITH RECTANGULAR SECTION

(g) Spanwise twisting moments

Moment point	Spanwise twisting moments, in-lb/lb, at loading point -											
	51	53	55	57	71	73	75	77	91	93	95	97
22	-1.67	-1.01	-0.65	-0.33	-3.00	-2.42	-1.82	-1.32	-4.44	-3.90	-3.33	-2.67
24	-.79	-.46	0	.30	-1.60	-1.20	-.74	-.22	-2.46	-2.04	-1.62	-1.17
26	-.22	.04	.35	1.10	-.48	-.16	.18	.62	-.75	-.42	-.09	.27
43	-4.26	-2.34	-.24	.45	-8.66	-6.26	-3.52	-1.34	-12.96	-10.32	-7.71	-4.68
45	-3.05	-2.43	-1.33	.72	-6.56	-5.30	-4.00	-1.88	-9.96	-8.52	-7.20	-5.55
63	-1.02	-.92	-.49	.16	-6.18	-3.88	-1.46	-.38	-12.03	-9.33	-5.76	-2.88
65	-1.53	-.35	-.06	.32	-5.42	-4.02	-2.10	.48	-9.90	-8.10	-6.30	-3.00
83	.47	-.23	-.12	.06	-1.36	-.96	-.60	.12	-7.95	-5.13	-1.53	-.21
85	-.81	-.28	-.31	-.06	-3.10	-1.64	-.84	-.12	-7.56	-6.48	-4.17	-.33

TABLE 2

WING WITH BICONVEX SECTION

(a) Deflections

Deflection point	Deflection, in./kip, at loading point -																
	11	13	15	17	51	53	55	57	71	73	75	77	91	93	95	97	91 (a)
11	0.0315	0.0118	0.0064	0.0046	-0.0127	-0.0109	-0.0096	-0.0084	-0.0244	-0.0226	-0.0210	-0.0194	-0.0363	-0.0351	-0.0336	-0.0314	-0.0339
13		.0128	.0076	.0064	-.0085	-.0082	-.0078	-.0073	-.0170	-.0166	-.0160	-.0156	-.0255	-.0252	-.0249	-.0243	-.0255
15			.0129	.0120	-.0068	-.0071	-.0076	-.0080	-.0134	-.0138	-.0144	-.0148	-.0201	-.0207	-.0210	-.0214	-.0204
17				.0327	-.0063	-.0075	-.0088	-.0115	-.0126	-.0138	-.0154	-.0172	-.0189	-.0204	-.0216	-.0230	-.0186
51					.0567	.0317	.0196	.0120	.1004	.0749	.0548	.0380	.1397	.1182	.0954	.0741	.2025
53						.0319	.0220	.0158	.0620	.0562	.0486	.0404	.0898	.0828	.0752	.0672	.1149
55							.0275	.0206	.0384	.0400	.0424	.0425	.0557	.0574	.0590	.0600	.0636
57								.0314	.0228	.0280	.0339	.0429	.0330	.0392	.0452	.0508	.0318
71									.2428	.1693	.1196	.0799	.3630	.2924	.2260	.1687	.4200
73										.1460	.1123	.0845	.2576	.2289	.1934	.1603	.2985
75											.1072	.0904	.1810	.1719	.1642	.1519	.1998
77												.1032	.1202	.1274	.1340	.1446	.1224
91													.6468	.4822	.3632	.2652	.7038
93														.4173	.3344	.2614	.5256
95															.3096	.2558	.3918
97																.2646	.2742

[a] Rear spar carries no shear from point 51 to point 31.

TABLE 2.- Continued

WING WITH BICONVEX SECTION

(b) Spanwise shears

Shear point	Spanwise shear, lb/lb, at loading point -												
	51	53	55	57	71	73	75	77	91	93	95	97	91 (a)
21	-0.053	-0.017	-0.003	0.004	-0.073	-0.048	-0.023	-0.006	-0.103	-0.080	-0.058	-0.032	-0.027
23	-.006	-.022	0	.004	-.051	-.050	-.049	-.027	-.091	-.087	-.083	-.081	-.173
25	.022	.013	-.007	.047	.045	.037	.027	.014	.074	.065	.058	.049	.046
27	.035	.025	.010	-.055	.077	.061	.044	.018	.119	.099	.080	.063	.152
41	.701	.276	.075	-.031	.645	.413	.194	.004	.682	.468	.266	.069	.001
43	.282	.492	.297	.131	.428	.400	.344	.268	.477	.416	.353	.304	1.307
45	.059	.196	.490	.404	.043	.192	.360	.489	.016	.172	.323	.466	.005
47	-.042	.037	.138	.496	-.115	-.006	.102	.239	-.175	-.057	.058	.161	-.314
61	-.150	.022	.001	-.017	.507	.187	.044	-.032	.374	.232	.100	-.005	.357
63	.058	-.104	.028	.006	.352	.470	.258	.083	.501	.400	.289	.176	.654
65	.083	.021	-.087	.119	.174	.254	.491	.413	.193	.294	.404	.476	.184
67	0	.054	.052	-.111	-.028	.088	.207	.534	-.061	.075	.201	.355	-.186
81	0	-.002	-.002	0	-.121	-.005	-.007	-.006	.401	.077	.001	-.008	.417
83	-.020	-.013	-.003	-.005	-.039	-.105	.008	-.013	.364	.544	.220	.064	.403
85	-.007	-.007	-.010	.005	.087	.016	-.081	.083	.177	.236	.568	.333	.186
87	.019	.017	.010	-.003	.053	.079	.069	-.075	.076	.145	.203	.609	.029

[a]Rear spar carries no shear from point 51 to point 31.

TABLE 2.- Continued

WING WITH BICONVEX SECTION

(c) Chordwise shears

Shear point	Chordwise shear, lb/lb, at loading point -												
	51	53	55	57	71	73	75	77	91	93	95	97	91 (a)
12	0.052	0.017	0.003	-0.004	0.072	0.048	0.022	0.006	0.101	0.078	0.057	0.031	0.026
14	.058	.038	.003	-.008	.124	.098	.070	.032	.194	.166	.139	.113	.197
16	.035	.025	.010	-.055	.077	.061	.044	.018	.119	.100	.081	.064	.153
52	-.160	.255	.074	-.014	.141	.227	.151	.035	.316	.243	.164	.075	-.356
54	.069	-.160	.341	.114	.216	.154	.240	.218	.288	.253	.230	.201	.311
56	.041	.017	-.085	.399	.083	.091	.104	.296	.110	.132	.144	.191	.128
72	-.150	.024	.003	-.017	-.396	.193	.052	-.025	-.024	.155	.101	.004	-.052
74	-.072	-.065	.034	-.008	-.006	-.250	.304	.071	.120	.013	.168	.117	.213
76	.018	-.038	-.044	.108	.079	-.008	-.139	.400	.131	.068	.002	.261	.207
92	.002	-.001	-.001	0	-.116	-.001	-.005	-.005	-.642	.081	.006	-.004	-.641
94	-.017	-.013	-.003	-.004	-.150	-.102	.005	-.015	-.269	-.396	.231	.063	-.231
96	-.021	-.018	-.012	.002	-.057	-.082	-.074	.070	-.082	-.153	-.213	.402	-.041

[a]Rear spar carries no shear from point 51 to point 31.

TABLE 2.- Continued

WING WITH BICONVEX SECTION

(d) Spanwise bending moments

Moment point	Spanwise bending moment, in-lb/lb, at loading point -												
	51	53	55	57	71	73	75	77	91	93	95	97	91 (a)
11	-2.04	-1.68	-1.45	-1.27	-3.84	-3.52	-3.22	-2.94	-5.70	-5.46	-5.16	-4.86	-5.10
13	-7.36	-7.24	-6.73	-6.43	-14.90	-14.60	-14.24	-13.74	-22.74	-22.26	-21.90	-21.51	-23.01
15	-5.66	-6.10	-6.57	-6.54	-11.36	-11.66	-12.16	-12.66	-16.95	-17.40	-17.82	-18.21	-17.31
17	-.89	-1.06	-1.32	-1.87	-1.72	-1.98	-2.22	-2.58	-2.58	-2.85	-3.03	-3.30	-2.46
$31^{(-)}$	-4.16	-2.77	-2.10	-1.59	-7.28	-6.24	-5.16	-4.30	-10.59	-9.72	-8.70	-7.62	-8.07
33	-7.22	-7.35	-6.18	-5.61	-15.66	-15.22	-14.68	-13.42	-24.12	-23.52	-22.89	-22.50	-26.40
35	-4.38	-5.05	-6.12	-4.87	-8.74	-9.44	-10.22	-11.16	-12.90	-13.53	-14.28	-14.94	-13.98
37	-.24	-.83	-1.60	-3.94	-.30	-1.10	-1.94	-3.12	-.39	-1.23	-2.10	-2.94	.45
$31^{(+)}$	2.91	.02	-1.33	-1.90	1.58	-.74	-2.34	-3.80	-.21	-2.22	-4.02	-5.52	-3.27
51	2.57	1.76	.36	-.37	6.22	2.64	.60	-.80	6.33	3.21	1.05	-.84	1.11
53	-.60	.48	.19	-.67	-6.82	-6.30	-5.14	-4.58	-13.86	-13.08	-12.33	-10.80	-12.66
55	-2.46	-1.25	-.37	-.64	-7.94	-7.86	-8.20	-6.72	-13.98	-14.04	-14.25	-14.73	-10.47
57	.31	-.39	-.83	-2.58	.66	-.76	-2.12	-4.90	.84	-.84	-2.28	-4.11	2.94
71	-.55	.29	.06	-.09	1.82	1.46	.28	-.30	6.54	1.53	-.03	-.54	5.91
73	1.82	.21	.31	.14	1.70	1.86	1.06	-.20	-3.96	-4.50	-3.36	-2.79	-5.07
75	-.60	-.16	-.25	.10	-3.08	-1.80	-.74	-.58	-8.04	-8.13	-9.21	-7.23	-6.84
77	.29	-.42	-.70	.19	.68	-.60	-1.44	-3.46	.87	-.96	-2.55	-6.54	2.58
97	.12	-.04	-.10	.16	.60	-.14	-.56	.14	1.56	.48	-.39	-4.53	1.83

[a]Rear spar carries no shear from point 51 to point 31.

TABLE 2.- Continued

WING WITH BICONVEX SECTION

(e) Chordwise bending moments

Moment point	Chordwise bending moment, in-lb/lb, at loading point -												
	51	53	55	57	71	73	75	77	91	93	95	97	91 (a)
13	-0.43	-0.57	-0.55	-0.44	-1.06	-1.12	-1.16	-1.14	-1.65	-1.68	-1.71	-1.80	-2.10
15	-.51	-.57	-.59	-.28	-1.12	-1.12	-1.12	-1.10	-1.68	-1.68	-1.68	-1.68	-1.98
51	-2.52	-1.73	-.36	.36	-6.14	-2.58	-.60	.80	-6.15	-3.15	-1.02	.84	-.96
53	-6.45	2.55	.32	.55	-13.38	-6.78	-1.58	.72	-18.57	-12.81	-6.93	-2.37	-22.80
55	-4.50	-1.32	4.75	.34	-10.08	-5.96	-1.66	1.72	-15.06	-10.74	-6.36	-2.07	-20.73
57	-.30	.38	.83	2.58	-.66	.74	2.10	4.90	-.81	.78	2.25	4.08	-2.91
71	.58	-.28	-.06	.09	-1.72	-1.42	-.28	.28	-6.39	-1.47	.03	.57	-5.70
73	-.98	.10	-.01	-.04	-9.02	2.02	.22	.38	-17.91	-8.64	-1.50	.27	-17.61
75	-2.07	.45	.45	-.74	-8.16	-2.86	4.58	.22	-15.15	-9.15	-3.00	1.35	-16.38
77	-.28	.41	.71	-.18	-.74	.54	1.42	3.46	-.96	.81	2.52	6.54	-2.61
93	.04	-.01	-.02	.01	-1.84	0	-.08	-.08	-10.20	1.38	.12	0	-10.08
95	-.74	.08	-.02	-.15	-2.38	-.16	.30	-.62	-8.01	-3.48	3.96	.45	-7.83
97	-.13	.04	.12	-.15	-.64	.12	.58	-.14	-1.62	-.48	.39	4.56	-1.89

[a]Rear spar carries no shear from point 51 to point 31.

TABLE 2.- Continued

WING WITH BICONVEX SECTION

(f) Bending moments in spars

Moment point	Bending moment in spars, in-lb/lb, at loading point -												
	51	53	55	57	71	73	75	77	91	93	95	97	91 (a)
41	-1.84	-0.76	-0.23	0.09	-4.96	-3.06	-1.72	-0.68	-7.08	-5.43	-3.69	-2.25	-7.08
61	1.01	.24	.12	.07	-.38	.14	.14	.14	-3.81	-1.92	-.99	-.39	-4.65
81	.02	.04	.03	.01	1.46	.12	.12	.10	-4.26	-.72	.09	.15	-4.41
53	-.26	.09	.05	.05	-.88	-.64	-.30	-.10	-1.50	-1.17	-.84	-.51	-1.35
73	.04	-.04	.01	.02	-.26	.08	.04	.04	-1.02	-.75	-.30	-.09	-.90
55	-.30	-.10	.18	.11	-.80	-.62	-.42	-.12	-1.32	-1.11	-.90	-.63	-1.41
75	-.11	-.02	-.03	.03	-.48	-.22	.12	.10	-1.05	-.81	-.63	-.21	-.96
47	-.81	-.76	-.67	.09	-1.68	-1.60	-1.58	-1.70	-2.46	-2.43	-2.34	-2.37	-2.88
67	-.89	-.29	.34	.86	-2.52	-1.74	-1.02	.30	-4.14	-3.36	-2.67	-2.31	-4.44
87	-.35	-.10	.05	-.19	-1.34	-.68	.06	.68	-2.85	-2.13	-1.65	-.57	-2.70

[a] Rear spar carries no shear from point 51 to point 31.

TABLE 2.- Concluded

WING WITH BICONVEX SECTION

(g) Spanwise twisting moments

Moment point	Spanwise twisting moment, in-lb/lb, at loading point -												
	51	53	55	57	71	73	75	77	91	93	95	97	91 (a)
22	-1.30	-0.84	-0.60	-0.37	-2.26	-1.92	-1.52	-1.22	-3.33	-3.00	-2.67	-2.28	-2.55
24	-1.05	-.63	-.08	.30	-2.10	-1.62	-1.12	-.50	-3.21	-2.73	-2.25	-1.74	-3.09
26	-.07	.16	.42	1.18	-.16	.14	.42	.82	-.24	.06	.36	.66	-.45
43	-5.89	-3.55	-.89	.18	-12.02	-9.02	-5.66	-2.98	-18.24	-14.97	-11.61	-7.95	-20.73
45	-4.10	-3.03	-1.40	.91	-8.76	-6.94	-5.10	-2.36	-13.14	-11.07	-9.12	-6.96	-16.38
63	-1.11	-.74	-.28	.46	-7.12	-4.36	-1.52	-.02	-14.04	-10.74	-6.57	-3.24	-11.25
65	-2.10	-.69	-.31	.17	-7.34	-5.40	-2.96	0	-13.50	-10.98	-8.58	-4.59	-11.70
83	.72	-.16	-.03	.13	-1.38	-.60	-.34	.38	-9.06	-5.67	-1.65	.09	-8.70
85	-.83	-.18	-.23	-.02	-3.18	-1.64	-.82	-.02	-8.64	-7.05	-4.35	-.15	-7.59

[a]Rear spar carries no shear from point 51 to point 31.

TABLE 3

SPECIAL CASES FOR WING WITH RECTANGULAR SECTION

(a) Deflections

Deflection point	[a]Case I		[b]Case II		[c]Case III	
	Deflection, in./kip, at loading point -		Deflection, in./kip, at loading point -		Deflection, in./kip, at loading point -	
	91	97	91	97	91	97
11	-0.0273	-0.0231	-0.0261	-0.0225	-0.0309	-0.0252
13	-.0213	-.0201	-.0213	-.0201	-.0213	-.0198
15	-.0159	-.0174	-.0165	-.0180	-.0156	-.0174
17	-.0126	-.0159	-.0123	-.0156	-.0135	-.0174
51	.0966	.0600	.0951	.0603	.0981	.0549
53	.0729	.0522	.0720	.0525	.0624	.0510
55	.0507	.0456	.0489	.0447	.0414	.0453
57	.0288	.0384	.0258	.0366	.0279	.0363
71	.2514	.1401	.2430	.1410	.2673	.1290
73	.2010	.1287	.1944	.1284	.1902	.1227
75	.1530	.1173	.1476	.1158	.1359	.1158
77	.1065	.1071	.1020	.1044	.0948	.1032
91	.4440	.2235	.4233	.2220	.4734	.2049
93	.3651	.2133	.3579	.2127	.3669	.2007
95	.2982	.2037	.2928	.2037	.2814	.1971
97	.2295	.1989	.2265	.1923	.2106	.1893

[a]Case I: Ribs rigid in bending only.

[b]Case II: Ribs rigid in bending and shear.

[c]Case III: No shear strain in ribs or spars.

TABLE 3.- Continued

SPECIAL CASES FOR WINGS WITH RECTANGULAR SECTION

(b) Spanwise shears

Shear point	[a]Case I		[b]Case II		[c]Case III	
	Spanwise shear, lb/lb, at loading point -		Spanwise shear, lb/lb, at loading point -		Spanwise shear, lb/lb, at loading point -	
	91	97	91	97	91	97
21	-0.208	-0.113	-0.252	-0.143	-0.190	-0.018
23	.029	.025	.014	.024	-.083	-.112
25	.104	.069	.170	.109	.098	-.008
27	.072	.017	.067	.010	.170	.134
41	.693	.233	.744	.239	1.042	.189
43	.521	.238	.534	.262	.165	.308
45	.110	.221	.097	.221	.005	.293
47	-.325	.308	-.376	.277	-.212	.210
61	.469	.097	.515	.081	.557	.042
63	.429	.159	.387	.151	.245	.205
65	.122	.233	.100	.245	.243	.251
67	-.012	.503	.011	.512	-.033	.499
81	.474	.003	.414	-.024	.531	-.008
83	.282	.067	.322	.086	.109	.096
85	.082	.193	.091	.282	.171	.193
87	.173	.725	.188	.647	.207	.706

[a]Case I: Ribs rigid in bending only.

[b]Case II: Ribs rigid in bending and shear.

[c]Case III: No shear strain in ribs or spars.

TABLE 3.- Continued

SPECIAL CASES FOR WING WITH RECTANGULAR SECTION

(c) Chordwise shears

Shear point	[a]Case I		[b]Case II		[c]Case III	
	Chordwise shear, lb/lb, at loading point -		Chordwise shear, lb/lb, at loading point -		Chordwise shear, lb/lb, at loading point -	
	91	97	91	97	91	97
12	0.206	0.113	0.249	0.143	0.185	0.016
14	.179	.086	.235	.120	.270	.127
16	.073	.018	.067	.010	.170	.134
52	.223	.133	.230	.154	.499	.148
54	.322	.211	.385	.266	.417	.250
56	.309	.196	.381	.241	.177	.293
72	.001	.094	.108	.106	.034	.047
74	.147	.183	.170	.169	.170	.154
76	.182	.223	.176	.137	.238	.213
92	-.584	.008	-.641	-.019	-.531	-.002
94	-.285	.081	-.306	.074	-.405	.103
96	-.187	.288	-.201	.361	-.221	.305

[a]Case I: Ribs rigid in bending only.

[b]Case II: Ribs rigid in bending and shear.

[c]Case III: No shear strain in ribs or spars.

TABLE 3.- Continued

SPECIAL CASES FOR WING WITH RECTANGULAR SECTION

(d) Spanwise bending moments

Moment point	[a]Case I		[b]Case II		[c]Case III	
	Spanwise bending moment, in-lb/lb, at loading point -		Spanwise bending moment, in-lb/lb, at loading point -		Spanwise bending moment, in-lb/lb, at loading point -	
	91	97	91	97	91	97
11	-11.64	-9.63	-11.43	-9.54	-12.18	-9.96
13	-18.27	-17.22	-18.33	-17.49	-17.64	-16.65
15	-13.41	-14.76	-13.65	-14.88	-12.78	-14.37
17	-4.68	-6.33	-4.62	-6.24	-5.31	-6.96
$31^{(-)}$	-18.06	-12.99	-18.90	-13.62	-20.46	-13.20
33	-17.13	-16.38	-17.58	-16.56	-16.98	-16.98
35	-11.19	-13.26	-10.59	-12.87	-9.45	-12.99
37	-1.62	-5.37	-.93	-4.95	-1.11	-4.83
$31^{(+)}$	-5.22	-7.65	-6.12	-8.25	-3.36	-8.67
51	6.60	-.09	7.20	-.06	9.09	-.54
53	-12.66	-10.44	-12.39	-10.53	-12.75	-10.05
55	-11.37	-12.36	-11.91	-12.33	-12.24	-12.66
57	1.98	-6.45	1.50	-6.48	-.69	-5.79
71	6.81	-.06	6.78	-.63	7.89	-.51
73	-2.94	-2.13	-2.49	-2.52	1.41	-2.13
75	-6.72	-6.66	-7.38	-6.78	-7.11	-6.84
77	.51	-8.31	-.12	-7.77	-.12	-7.53
97	1.98	-4.92	2.52	-4.32	2.67	-5.01

[a]Case I: Ribs rigid in bending only.

[b]Case II: Ribs rigid in bending and shear.

[c]Case III: No shear strain in ribs or spars.

TABLE 3.- Continued

SPECIAL CASES FOR WING WITH RECTANGULAR SECTION

(e) Chordwise bending moments

Moment point	[a]Case III	
	Chordwise bending moment, in-lb/lb, at loading point -	
	91	97
13	-2.37	-2.79
15	-1.32	-2.22
51	-8.91	.54
53	-14.58	-1.68
55	-10.29	-1.41
57	.63	5.79
71	-7.71	.51
73	-15.78	.33
75	-12.27	2.61
77	.03	7.50
93	-8.31	0
95	-6.84	1.17
97	-2.70	5.04

[a]Cases I and II were not measured. Case III: No shear strain in ribs or spars.

TABLE 3.- Continued

SPECIAL CASES FOR WING WITH RECTANGULAR SECTION

(f) Bending moments in spars

Moment point	[a]Case I		[b]Case II		[c]Case III	
	Bending moment in spar, in-lb/lb, at loading point -		Bending moment in spar, in-lb/lb, at loading point -		Bending moment in spar, in-lb/lb, at loading point -	
	91	97	91	97	91	97
41	-10.50	-5.16	-9.87	-5.04	-12.60	-4.32
61	-6.33	-1.20	-5.49	-1.23	-6.90	-.93
81	-5.10	.06	-4.41	.36	-5.67	.15
53	-.90	-.39	-.87	-.39	-1.08	-.33
73	-.60	-.12	-.63	-.12	-.78	-.09
55	-.87	-.42	-.84	-.45	-.90	-.42
75	-.66	-.18	-.69	-.21	-.78	-.15
47	-5.91	-4.02	-5.46	-3.81	-3.96	-4.35
67	-7.11	-3.78	-7.47	-3.87	-7.65	-4.29
87	-4.53	-1.35	-5.40	-1.35	-5.85	-1.05

[a]Case I: Ribs rigid in bending only.

[b]Case II: Ribs rigid in bending and shear.

[c]Case III: No shear strain in ribs or spars.

TABLE 3.- Concluded

SPECIAL CASES FOR WING WITH RECTANGULAR SECTION

(g) Spanwise twisting moments

Moment point	[a]Case I		[b]Case II		[c]Case III	
	Spanwise twisting moment, in-lb/lb, at loading point -		Spanwise twisting moment, in-lb/lb, at loading point -		Spanwise twisting moment, in-lb/lb, at loading point -	
	91	97	91	97	91	97
22	-3.15	-1.62	-3.51	-1.86	-5.43	-3.00
24	-2.43	-1.17	-2.94	-1.44	-3.33	-1.50
26	-1.86	-.72	-2.61	-1.14	-1.44	.03
43	-12.06	-4.95	-11.13	-4.56	-11.31	-4.05
45	-11.94	-4.95	-11.13	-4.50	-8.46	-4.89
63	-12.81	-3.24	-12.63	-3.60	-12.27	-3.18
65	-11.01	-2.37	-11.16	-2.79	-10.26	-3.39
83	-8.79	-.42	-9.09	-.03	-8.49	-.24
85	-8.28	-.30	-9.39	-.27	-8.70	-.39

[a]Case I: Ribs rigid in bending only.

[b]Case II: Ribs rigid in bending and shear.

[c]Case III: No shear strain in ribs or spars.

TABLE 4

SYMMETRIC VIBRATION MODES FOR WING WITH BICONVEX SECTION

Deflection point	Symmetric vibration modes at mode number -			
	1	2	3	4
	Frequency, cps			
	31.6	102.9	202	225
11	-0.95	1.24	8.60	-3.20
13	-.76	1.28	8.18	-3.72
15	-.74	1.58	10.00	-4.88
17	-.72	1.92	12.20	-6.22
51	2.81	1.39	-6.45	-7.98
53	2.15	-1.30	-4.28	-6.31
55	1.66	-3.08	-3.39	-3.34
57	1.27	-3.78	-3.90	.34
71	6.40	5.58	-7.01	-4.49
73	5.38	.58	-1.32	-4.31
75	4.45	-3.54	2.24	-2.40
77	3.59	-6.40	2.16	.39
91	10.00	10.00	-2.12	10.00
93	8.83	4.34	4.32	8.02
95	7.69	-1.22	9.24	6.57
97	6.59	-5.96	11.20	5.96

TABLE 5

SYMMETRIC VIBRATION MODES FOR WING WITH RECTANGULAR SECTION

Deflection point	Symmetric vibration modes at mode number -			
	1	2	3	4
	Frequency, cps			
	36.0	114.0	228	252
11	-0.86	0.94	10.00	-4.60
13	-.67	1.06	10.10	-5.82
15	-.56	1.28	11.00	-6.81
17	-.55	1.54	11.85	-7.40
51	2.70	1.30	-11.30	-6.60
53	2.07	-1.46	-8.40	-6.00
55	1.58	-3.12	-6.64	-2.70
57	1.14	-3.28	-6.14	1.71
71	6.30	5.30	-10.85	-3.24
73	5.28	.37	-3.38	-4.80
75	4.34	-3.79	2.40	-2.68
77	3.42	-6.00	.64	1.32
91	10.00	9.99	-.30	10.00
93	8.82	4.38	8.80	7.20
95	7.60	-1.51	16.85	5.03
97	6.40	-5.86	15.10	4.80

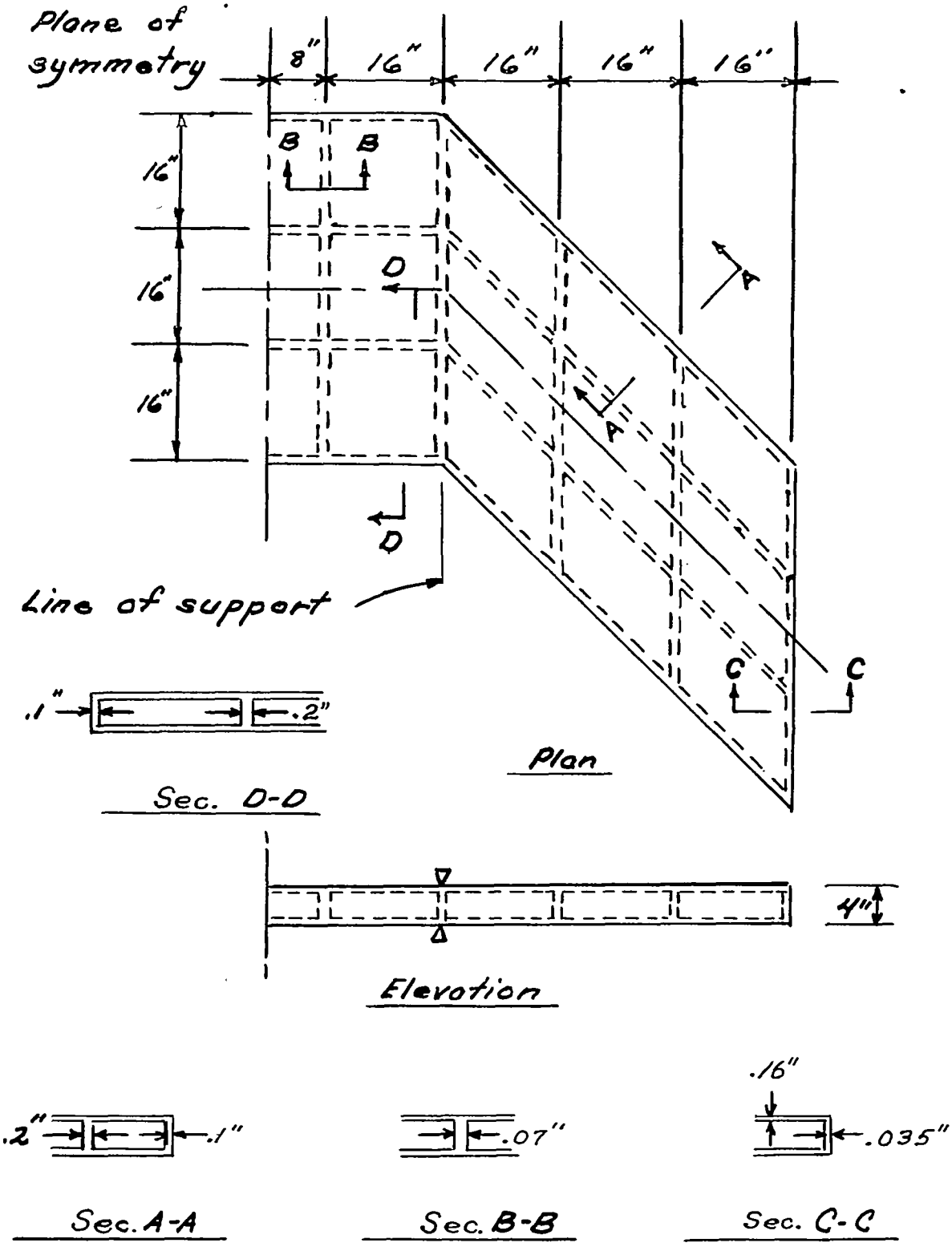

Figure 1.- Wing with rectangular section.

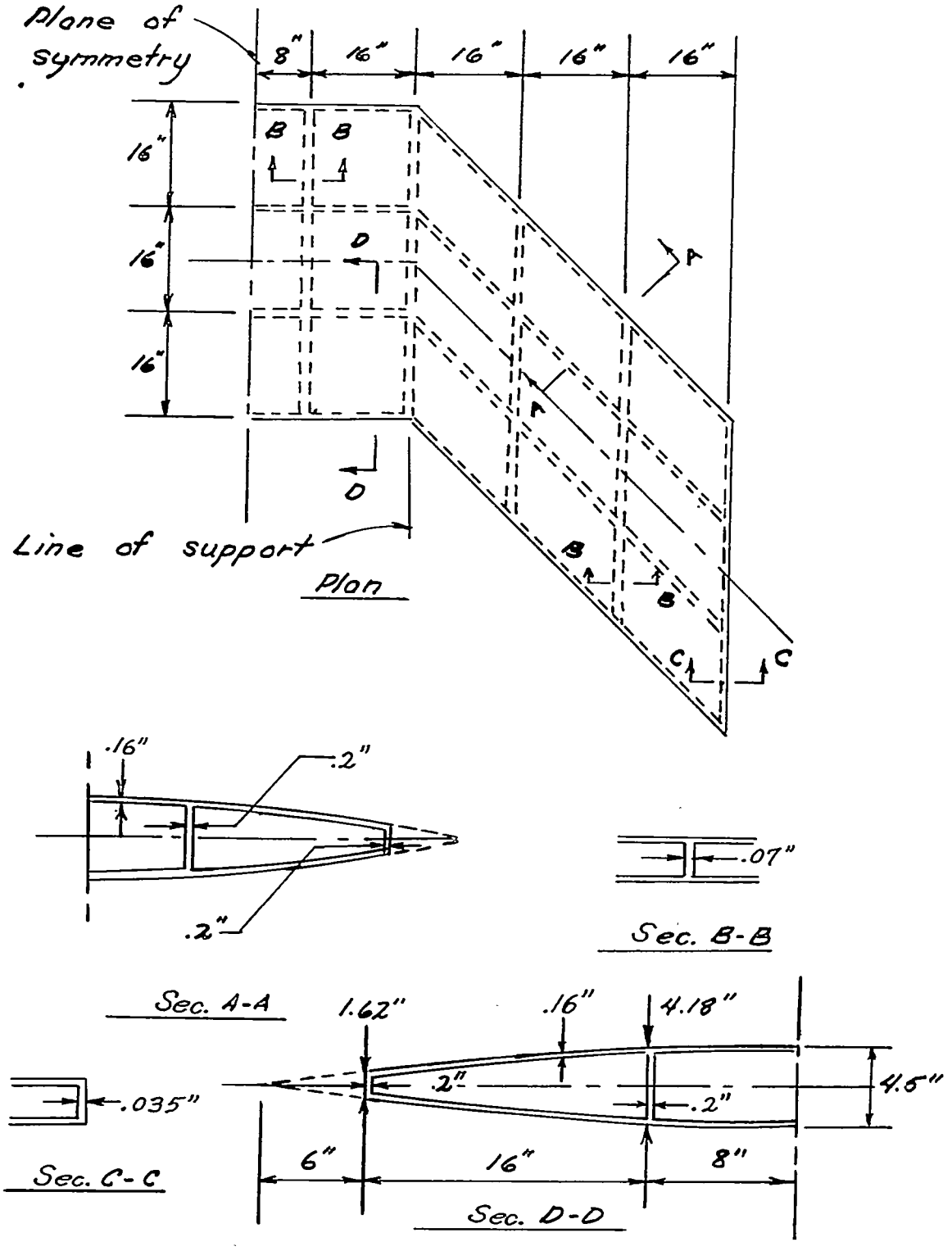

Figure 2.- Wing with biconvex section.

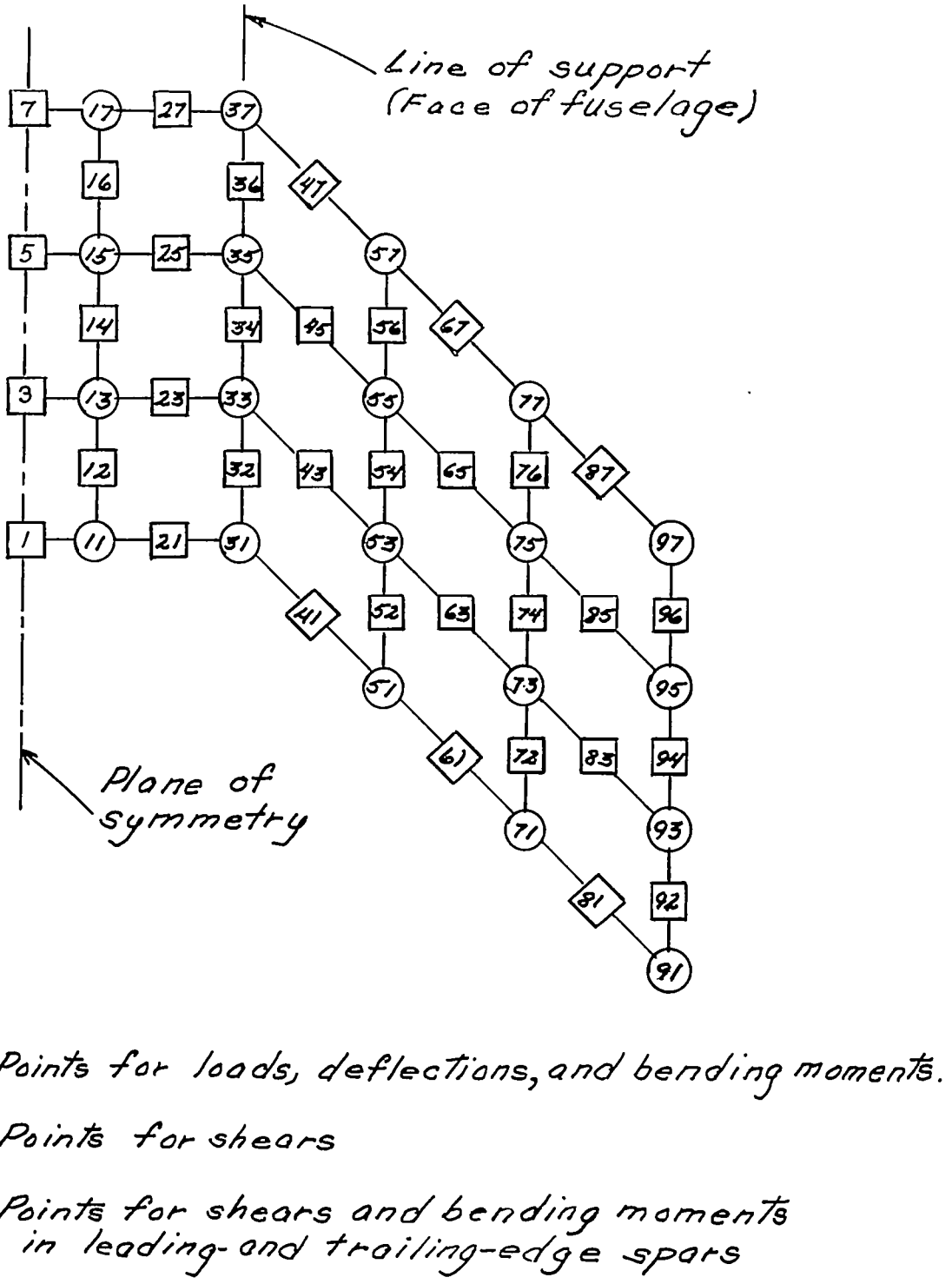

Figure 3.- Numbering of points where quantities are measured.

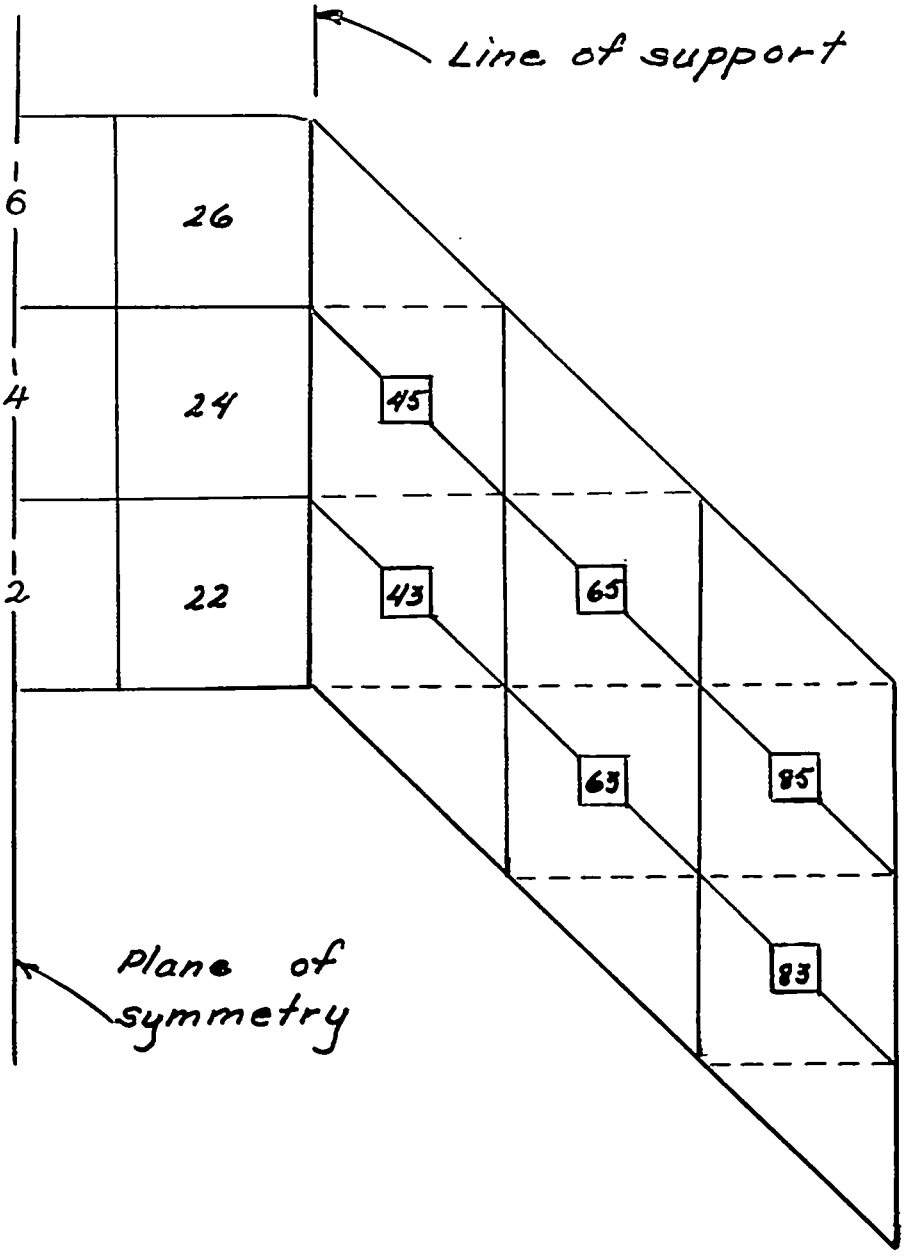

Figure 4.- Points at which twisting moments are measured.

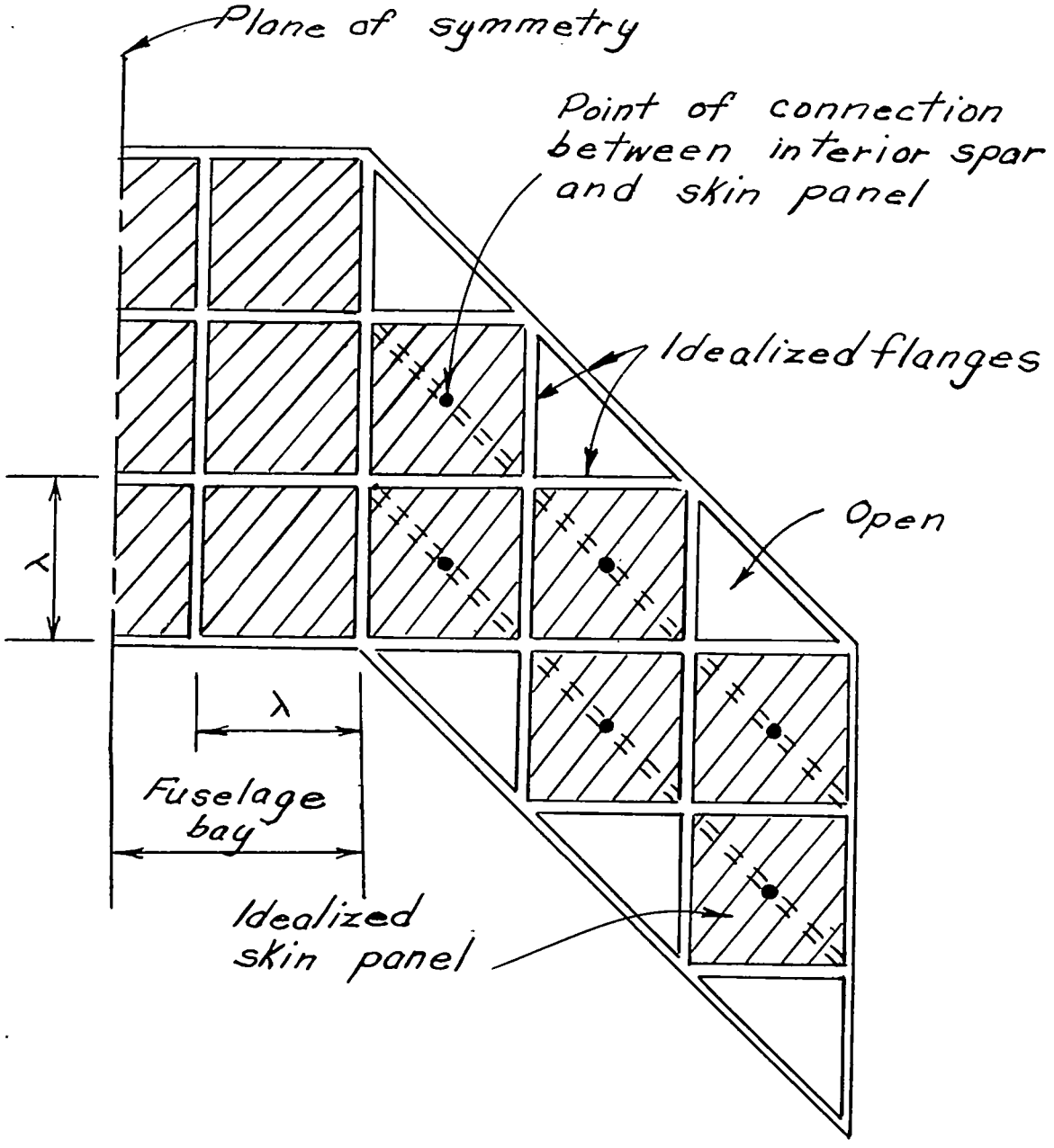

Figure 5.- Idealized skin.

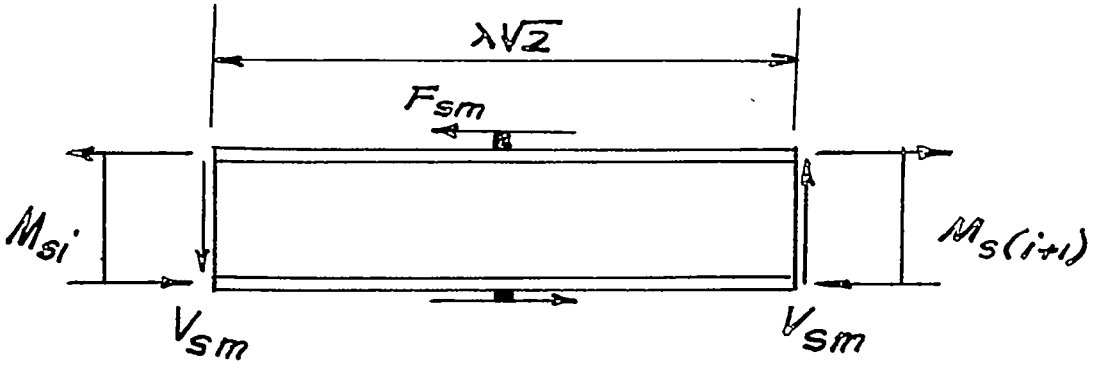

(a) Forces acting on one bay.

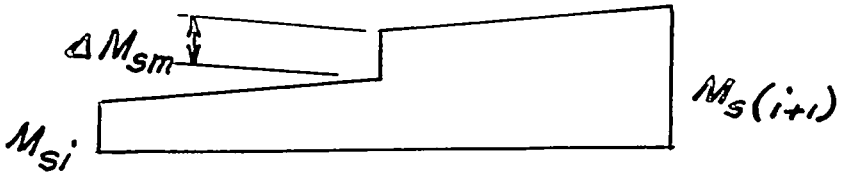

(b) Bending-moment diagram.

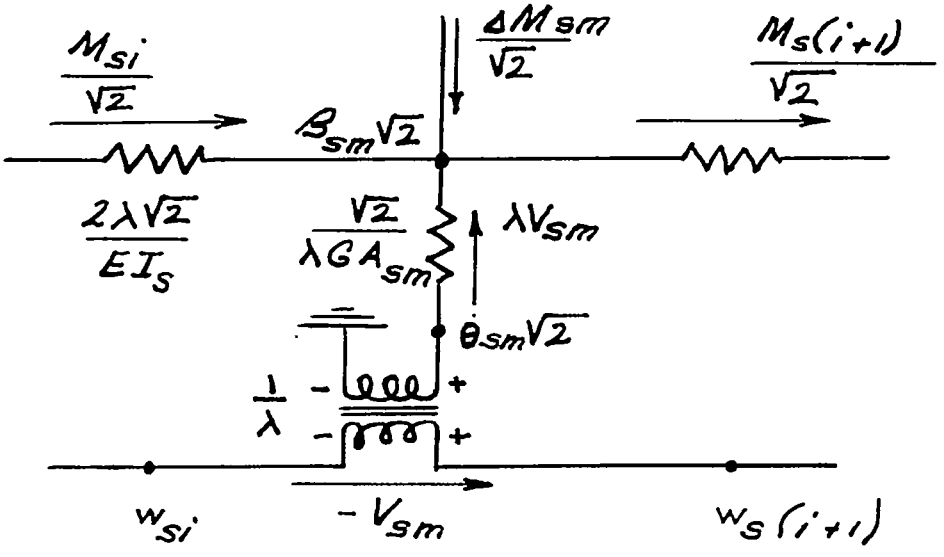

(c) Analogous circuit.

Figure 6.- Idealized interior spar and analogous circuit.

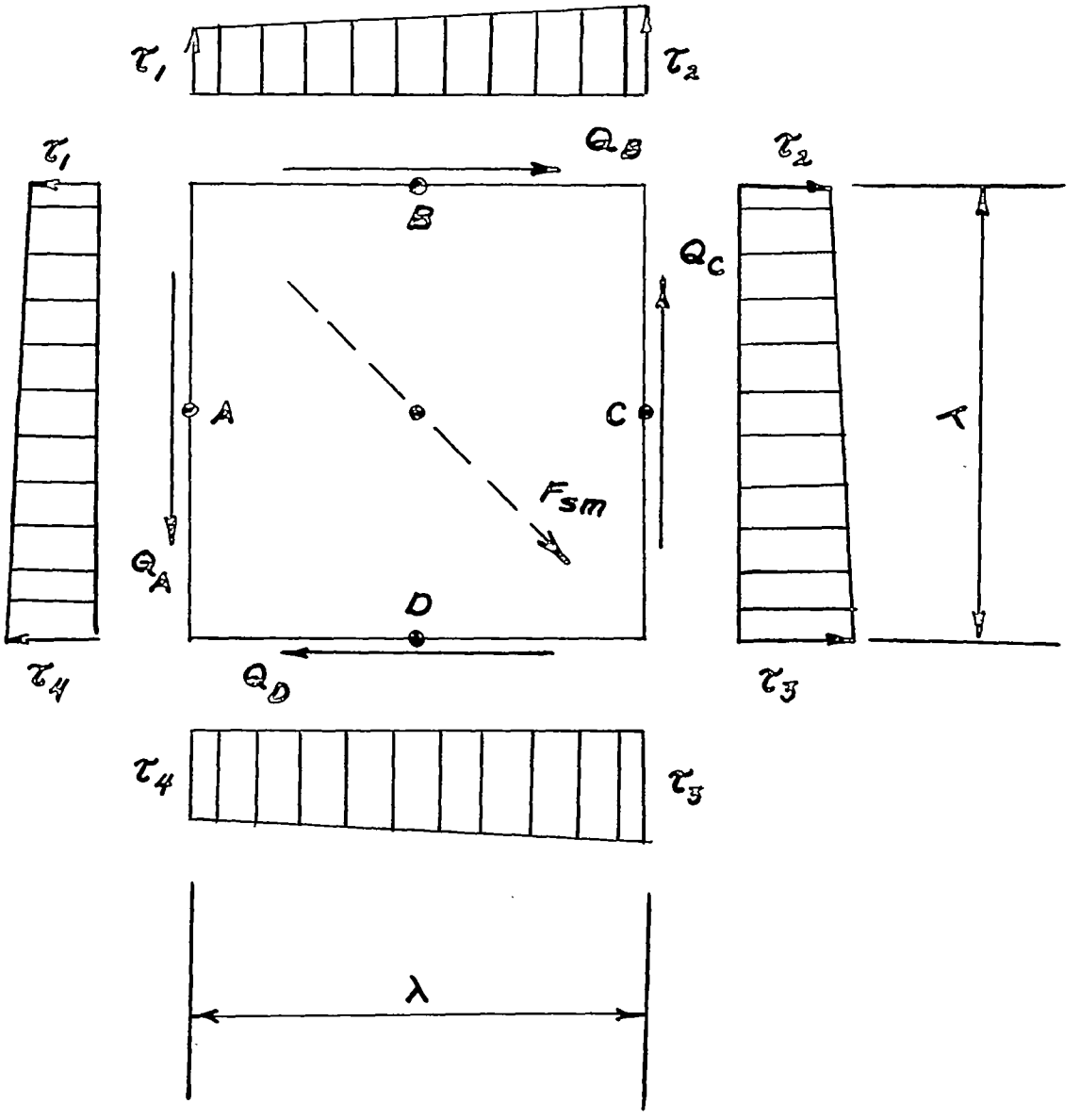

Figure 7.- Forces acting on idealized skin panel.

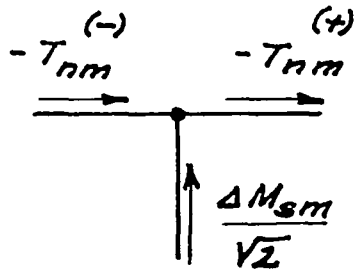

(a) Analogous to equation (15a).

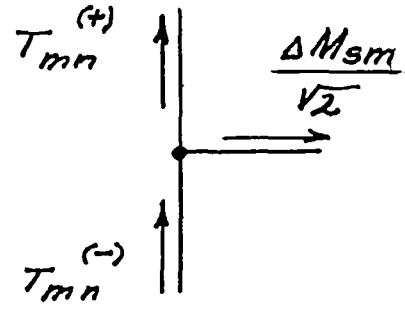

(b) Analogous to equation (15b).

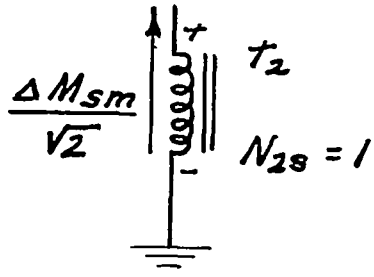

(c) Transformer for point in figure 8(a).

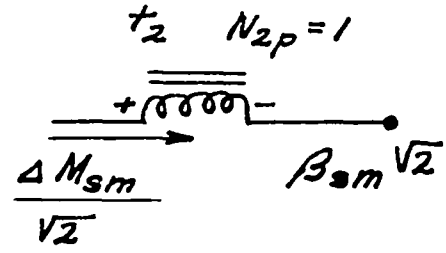

(d) Transformer for point in figure 8(b).

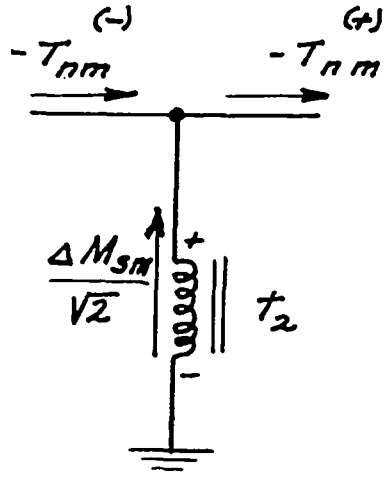

(e) Connected circuit for figures 8(a) and 8(c).

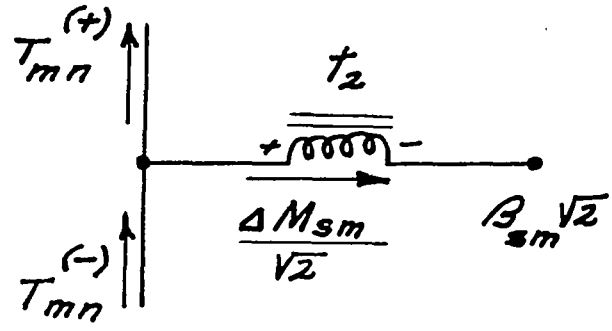

(f) Connected circuit for figures 8(b) and 8(d).

Figure 8.- Nodal points analogous to center point of skin panel.

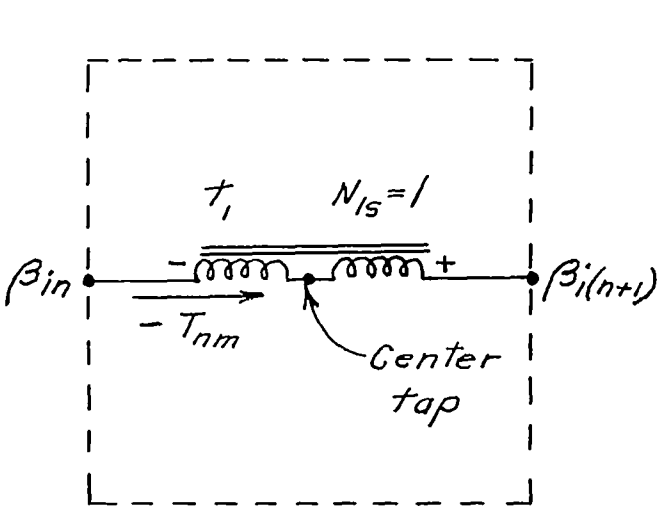

(a) Spanwise twisting moments.

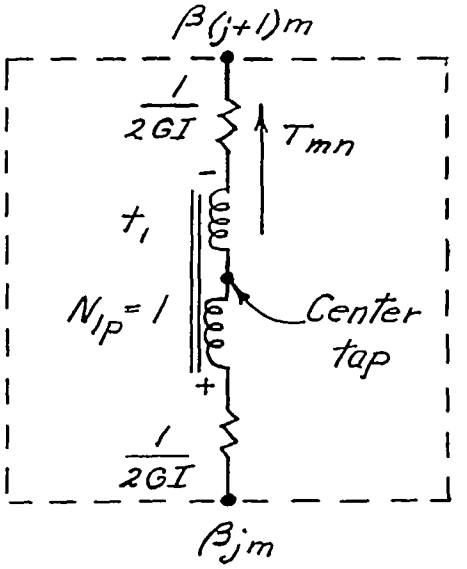

(b) Chordwise twisting moments.

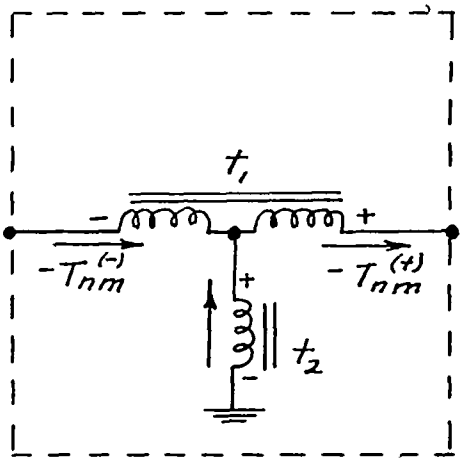

(c) Spanwise twisting moments with swept spar.

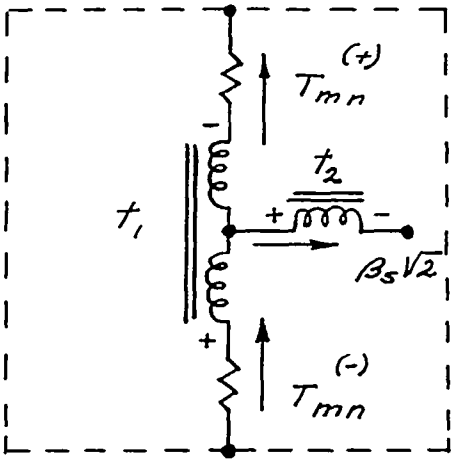

(d) Chordwise twisting moments with swept spar.

Figure 9.- Analogous circuits for twisting moments.

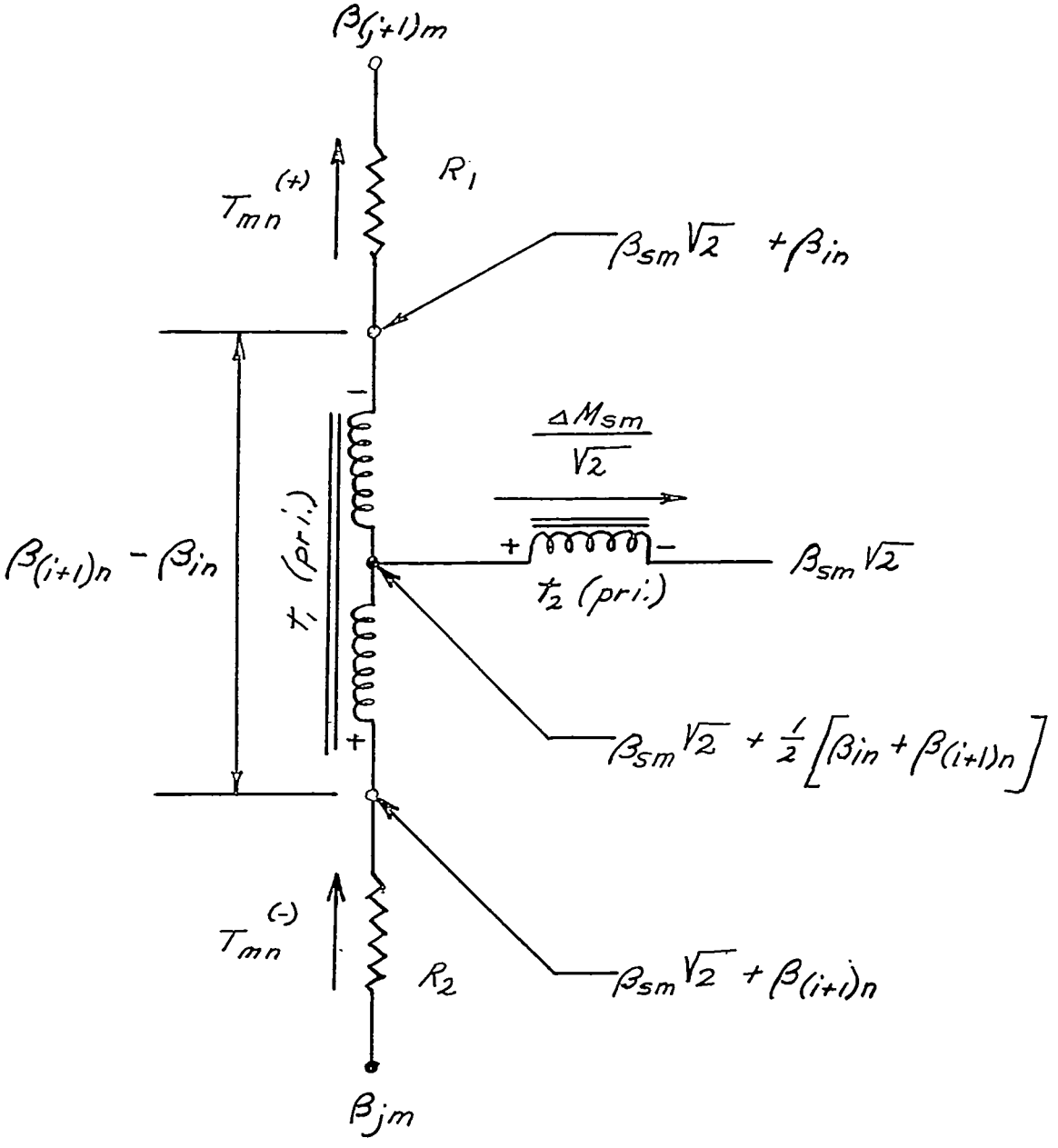

Figure 10.- Analogous circuits for chordwise twisting moments.

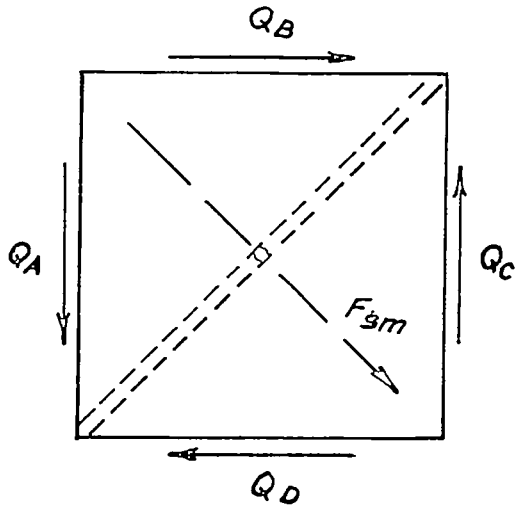

(a) Idealized skin panel.

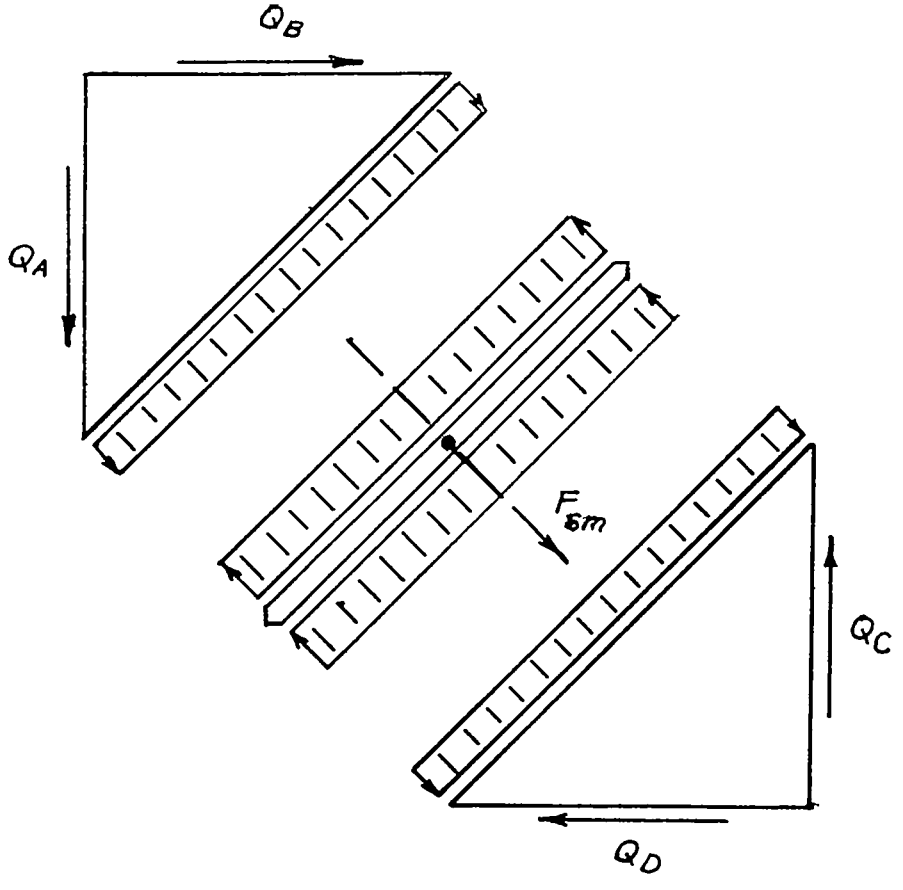

(b) Subdivided panel.

Figure 11.- Subdivision of idealized skin panel.

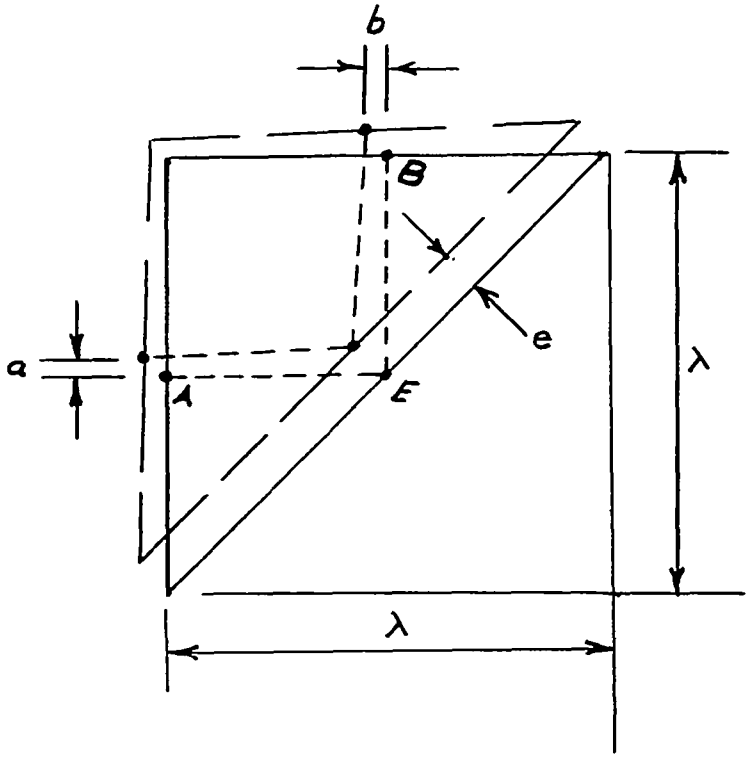

(a) Inboard triangle.

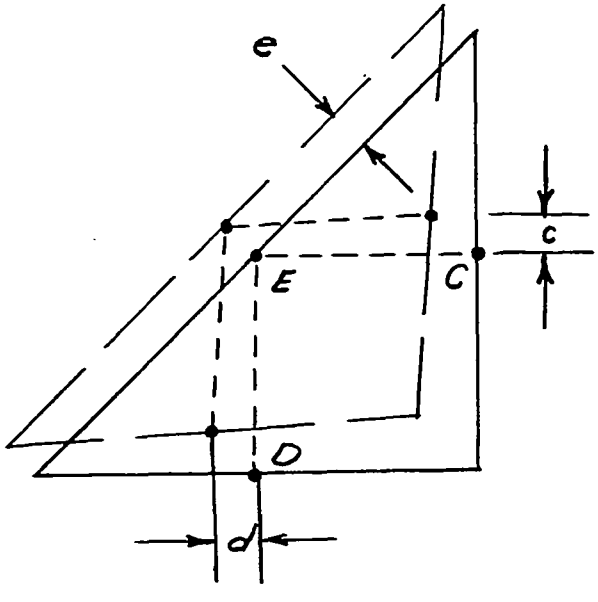

(b) Outboard triangle.

Figure 12.- Shearing strains in triangular panels.

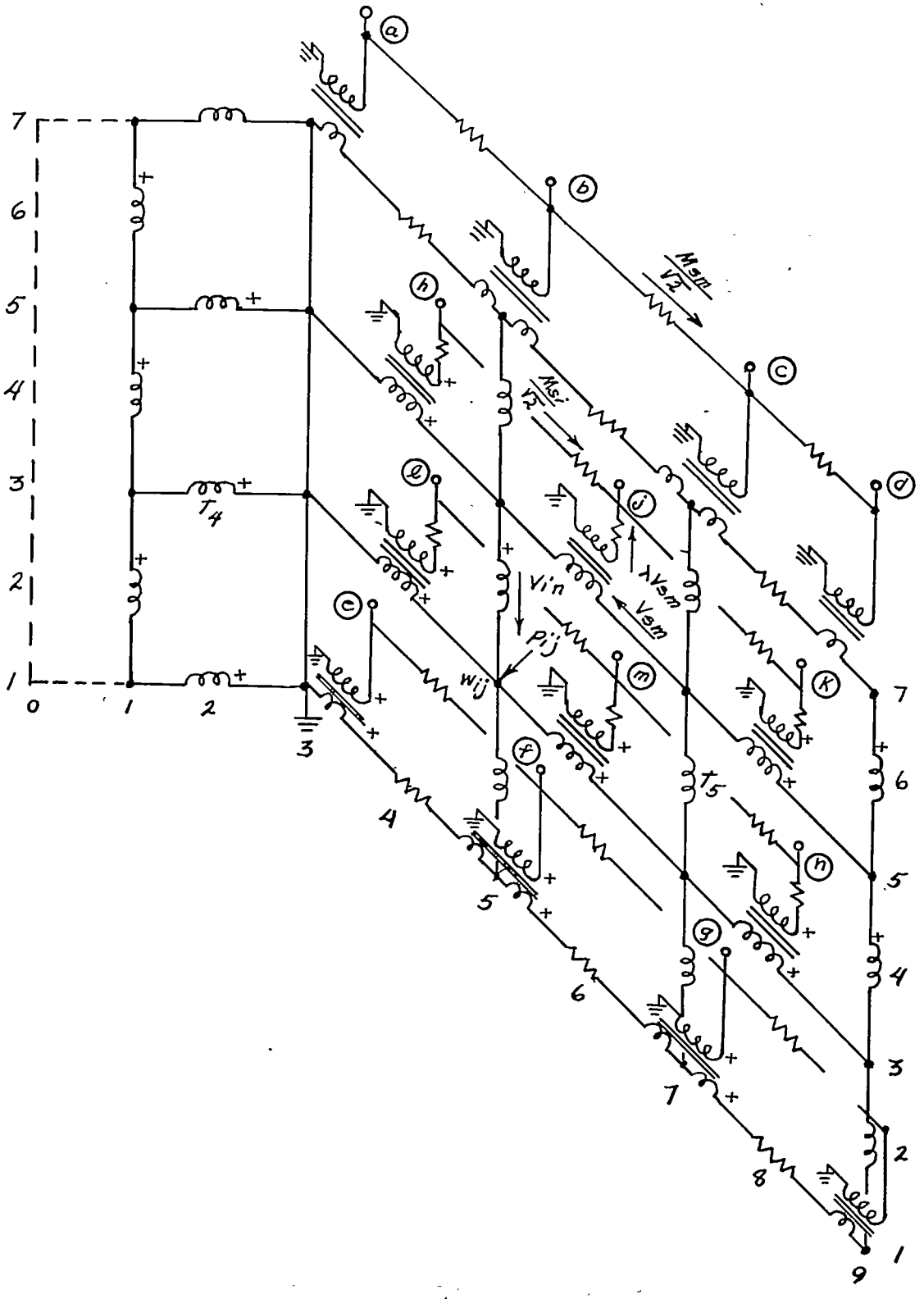

Figure 13.- Circuit for shears, deflections, and bending moments in spars.

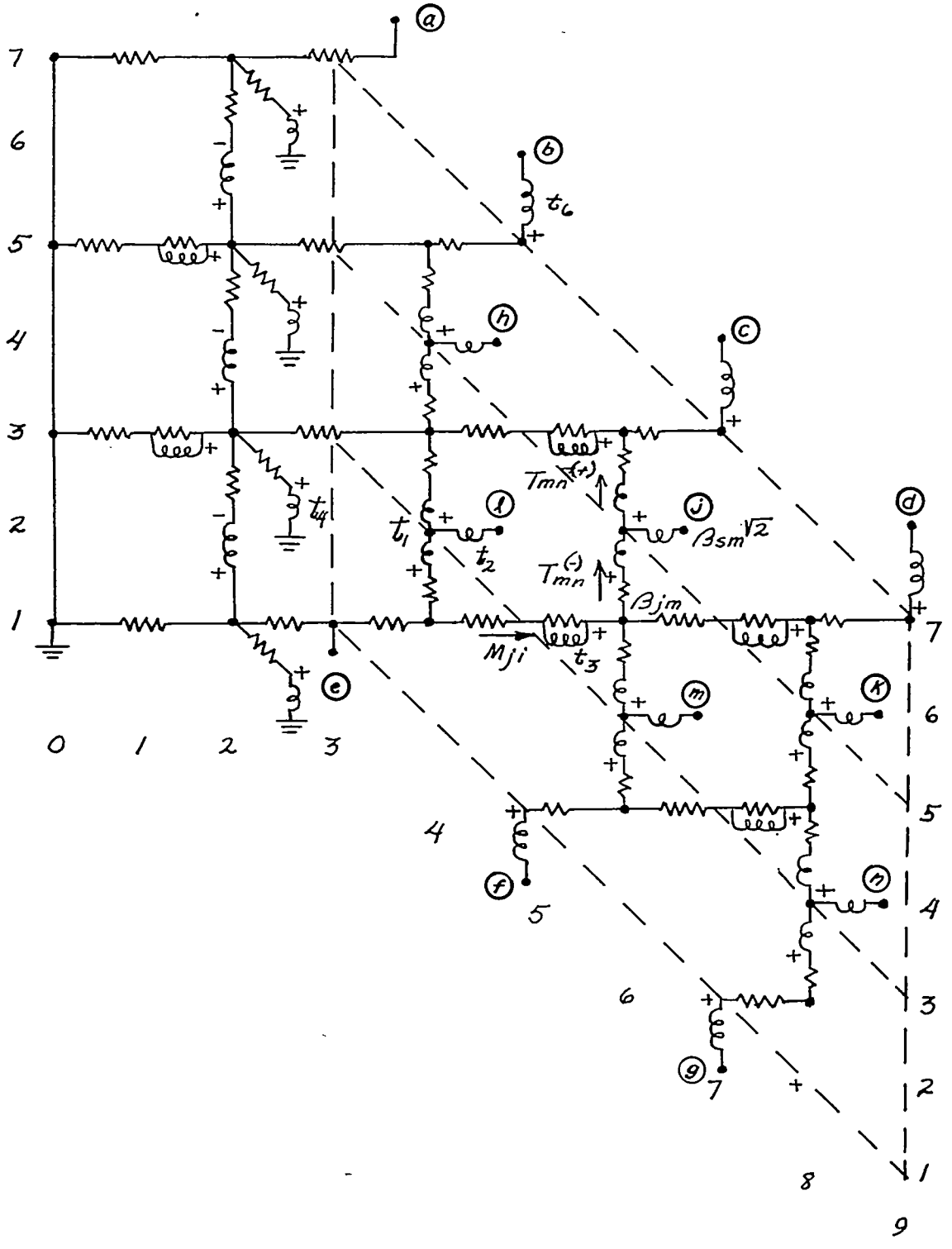

Figure 14.- Circuit for spanwise bending moments and chordwise twisting moments.

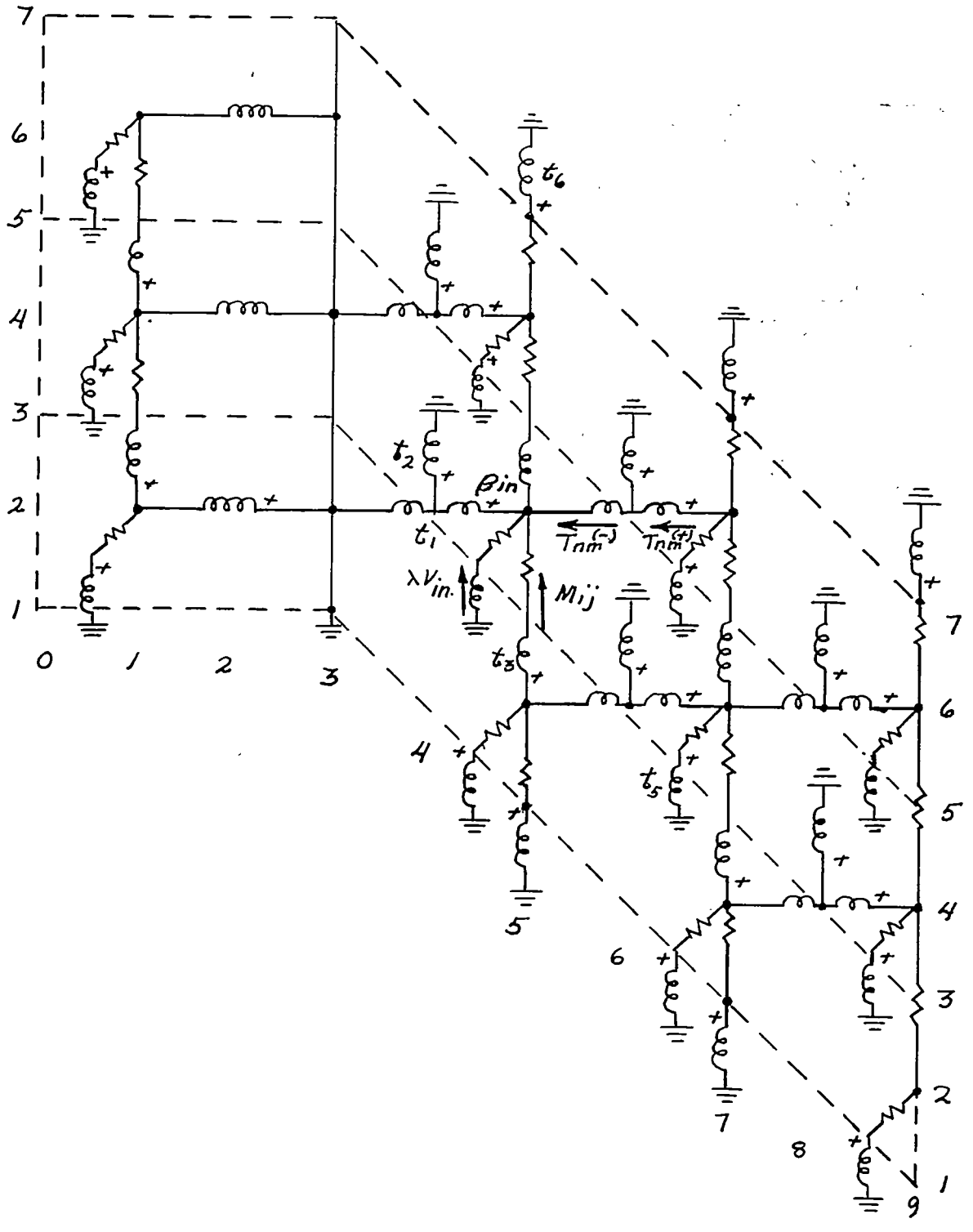

Figure 15.- Circuit for chordwise bending moments and spanwise twisting moments.

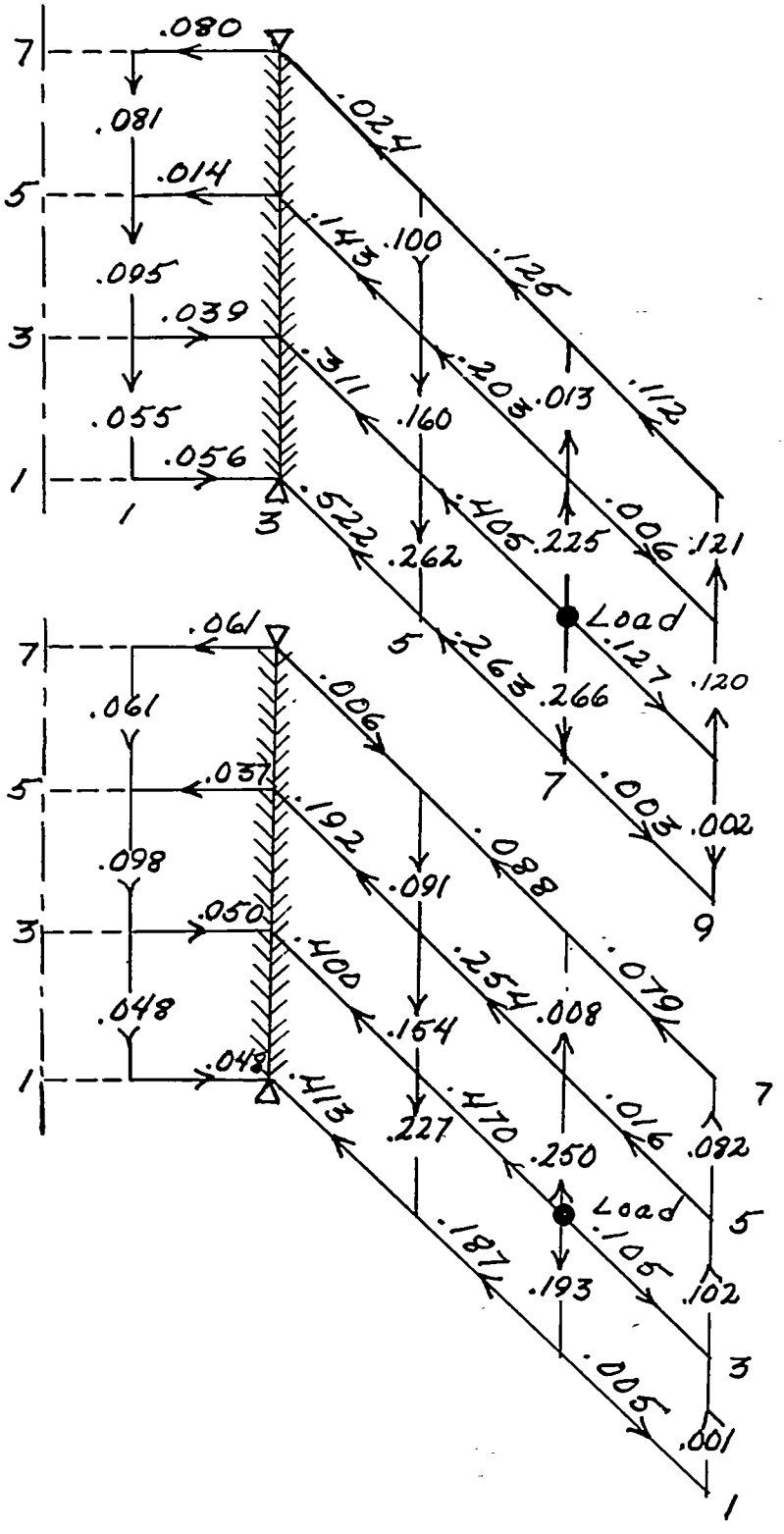

(a) Rectangular section.

(b) Biconvex section.

Figure 16.- Distribution of shears. Load at point 73.

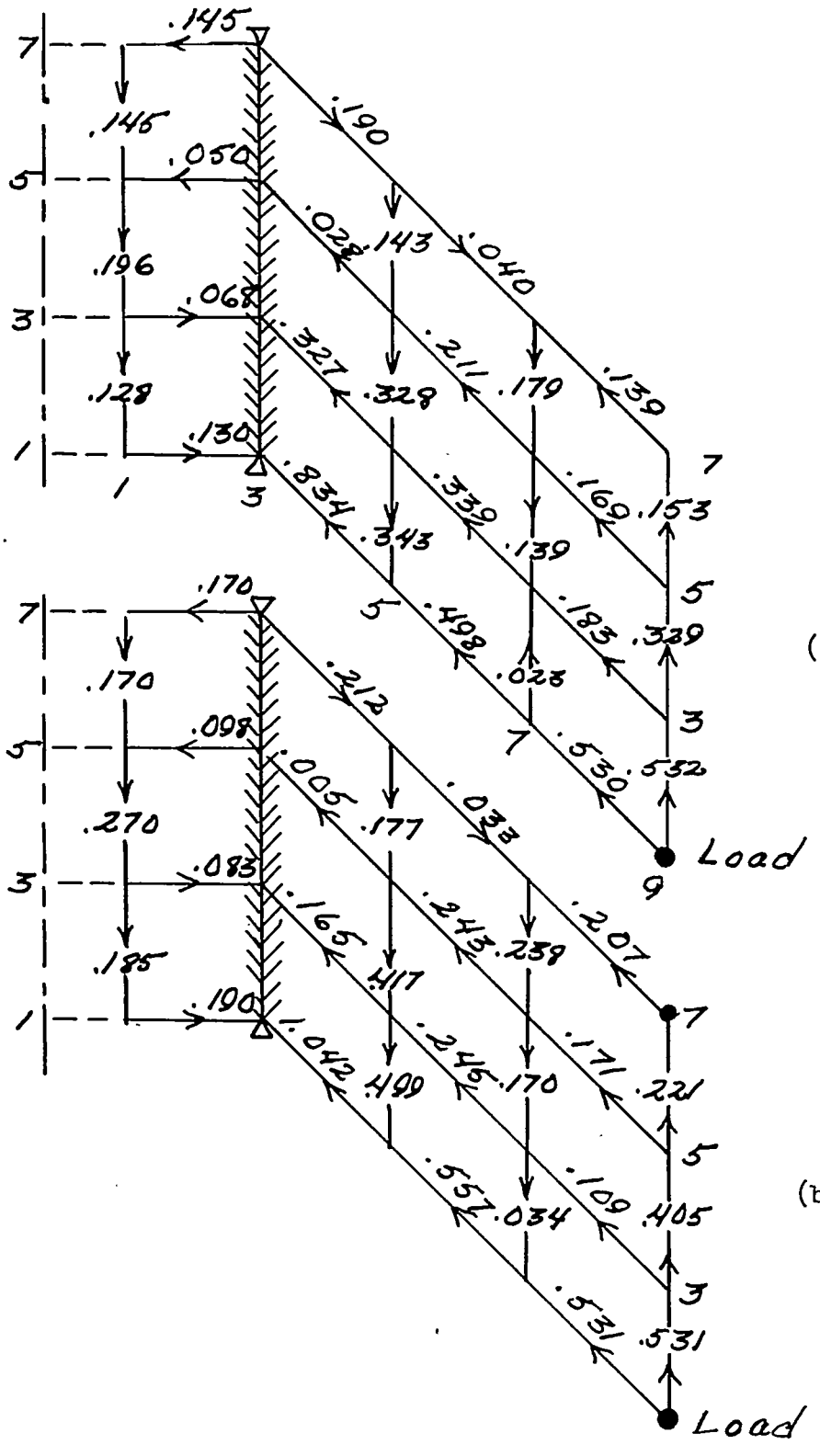

(a) Basic wing with shear strain in ribs and spars.

(b) Basic wing without shear strain in ribs and spars.

Figure 17.- Distribution of shears. Rectangular section; load at point 91.

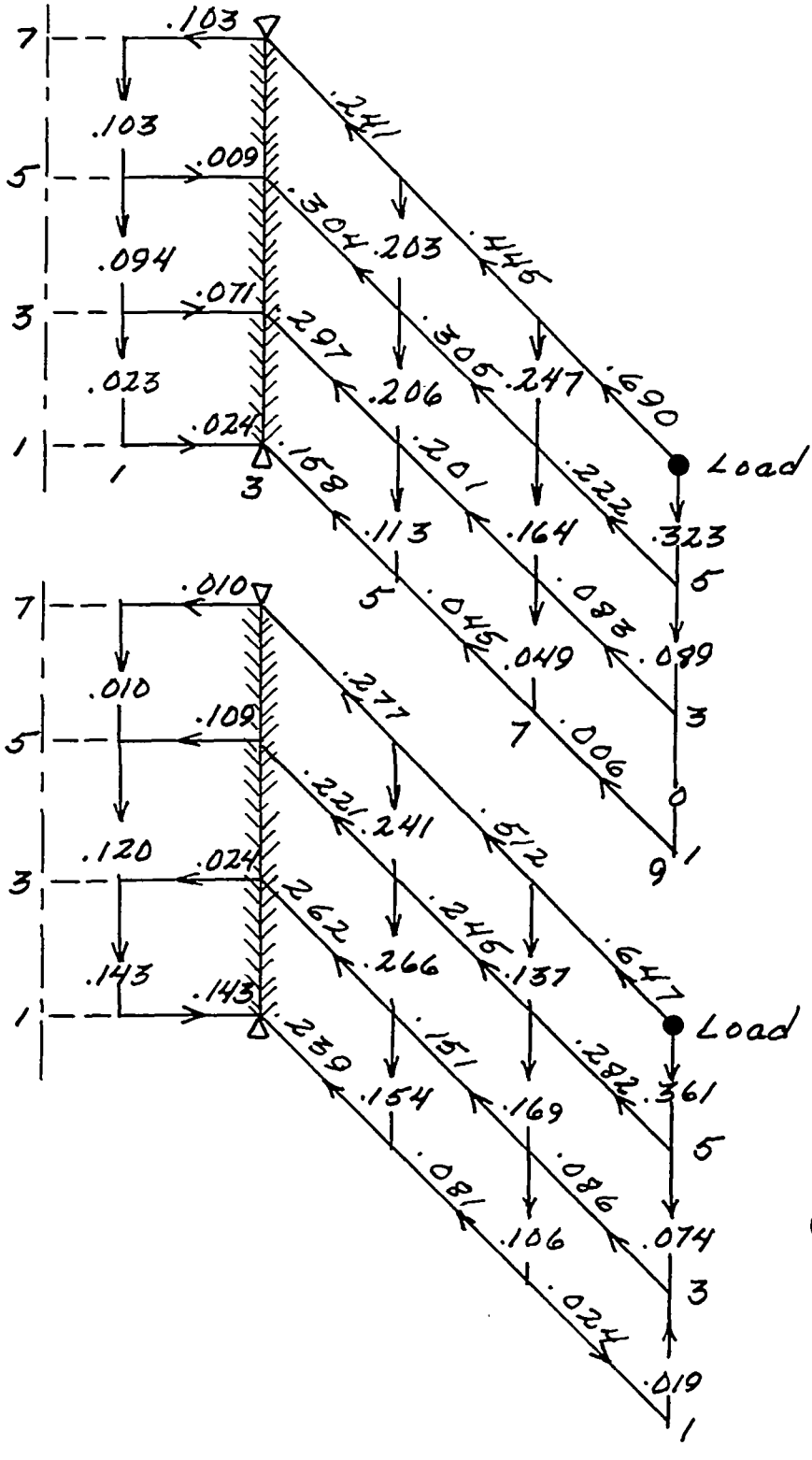

(a) Elastic ribs.

(b) Rigid ribs.

Figure 18.- Distribution of shears. Rectangular section; load at point 97.

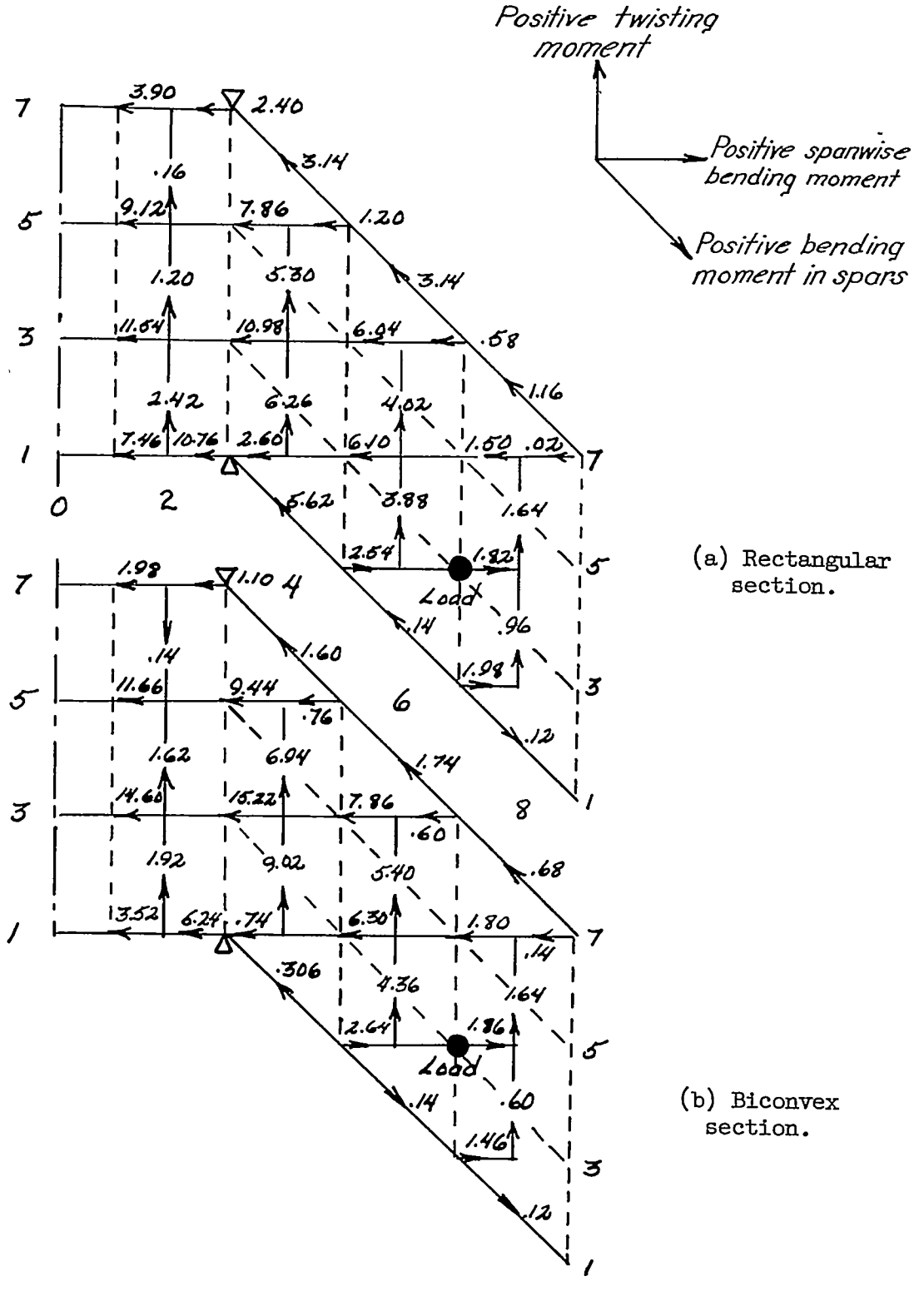

(a) Rectangular section.

(b) Biconvex section.

Figure 19.- Distribution of spanwise bending moments and chordwise twisting moments. Load at point 73.

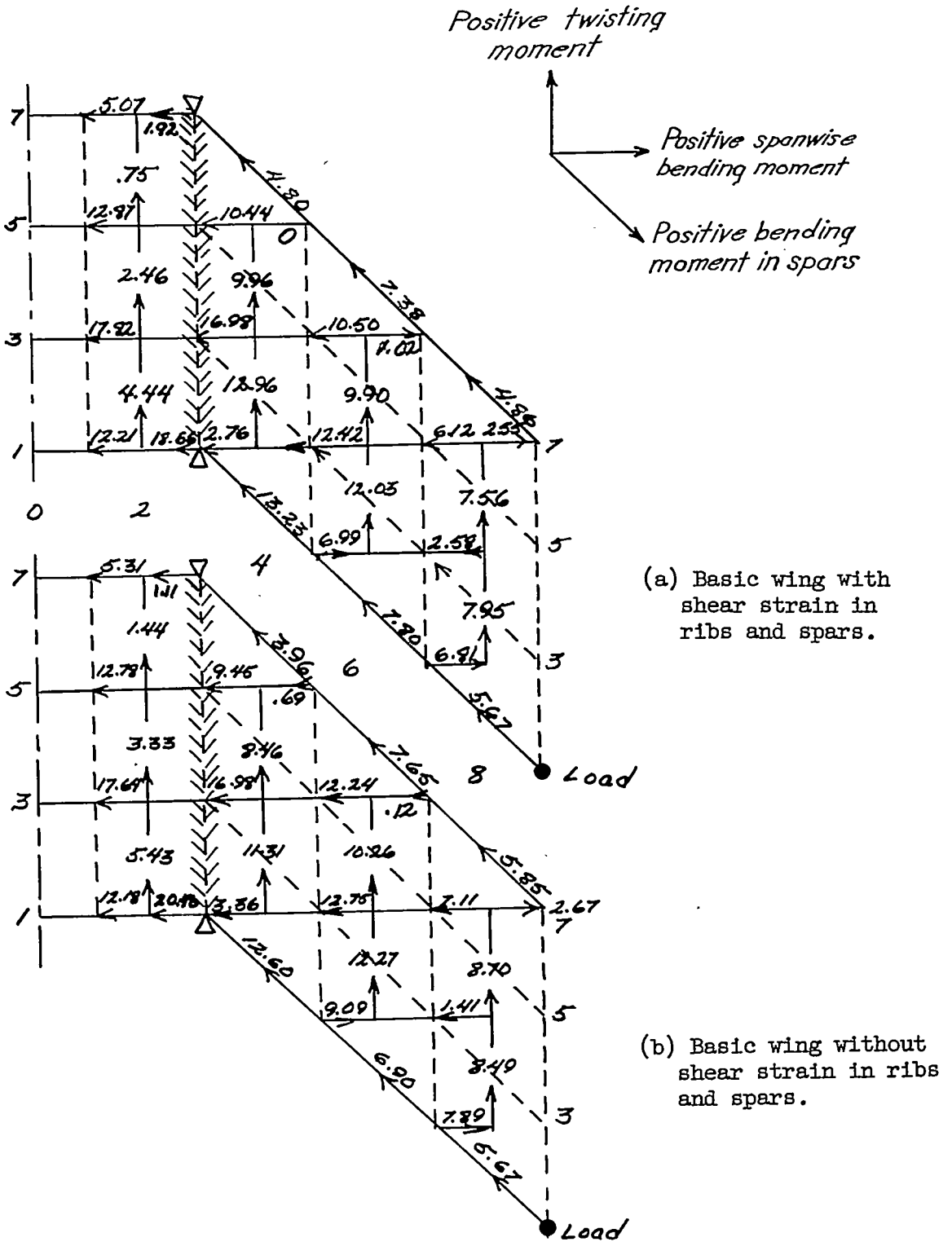

(a) Basic wing with shear strain in ribs and spars.

(b) Basic wing without shear strain in ribs and spars.

Figure 20.- Distribution of spanwise bending moments and chordwise twisting moments. Rectangular section; load at point 91.

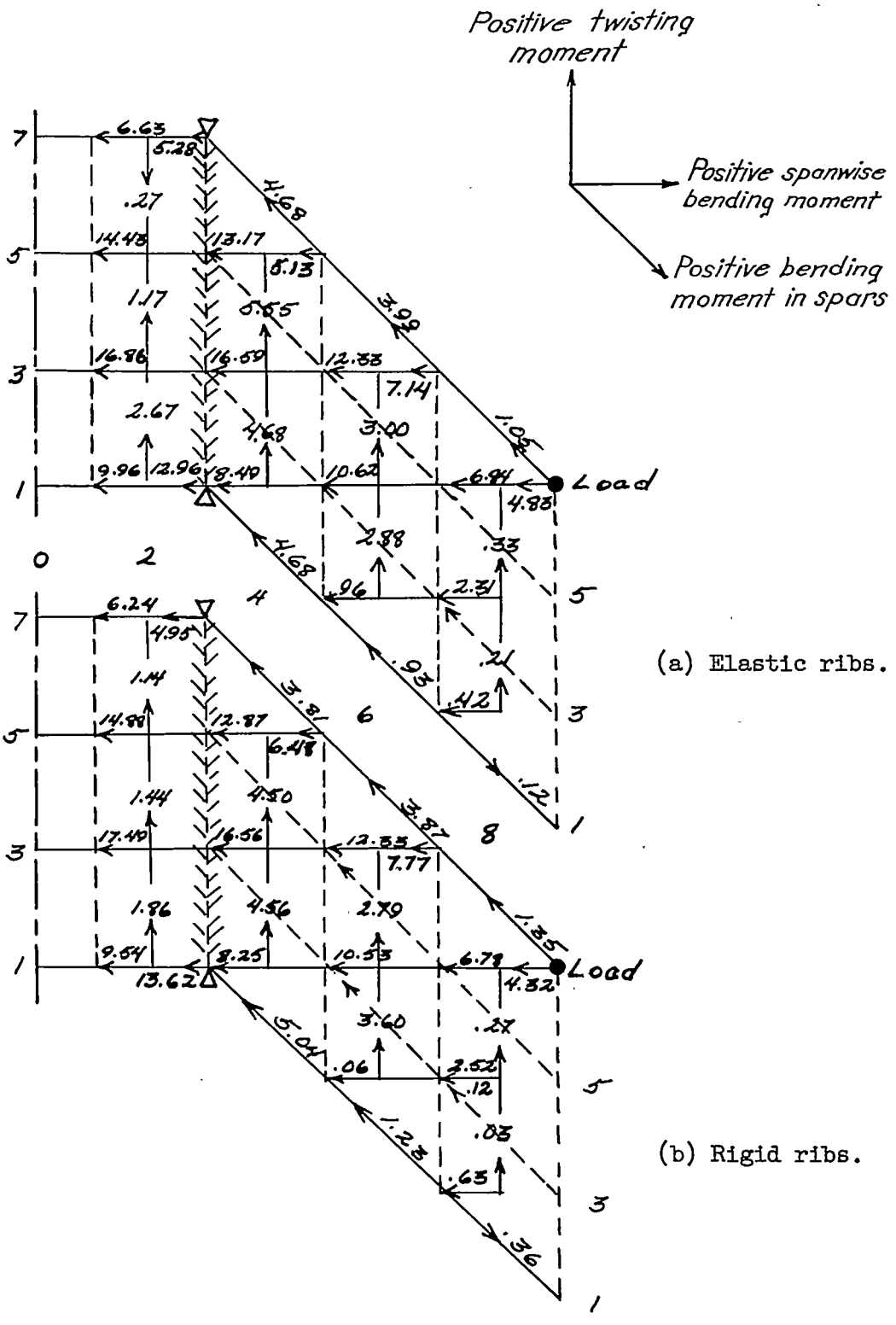

Figure 21.- Distribution of spanwise bending moments and chordwise twisting moments. Rectangular section; load at point 97.

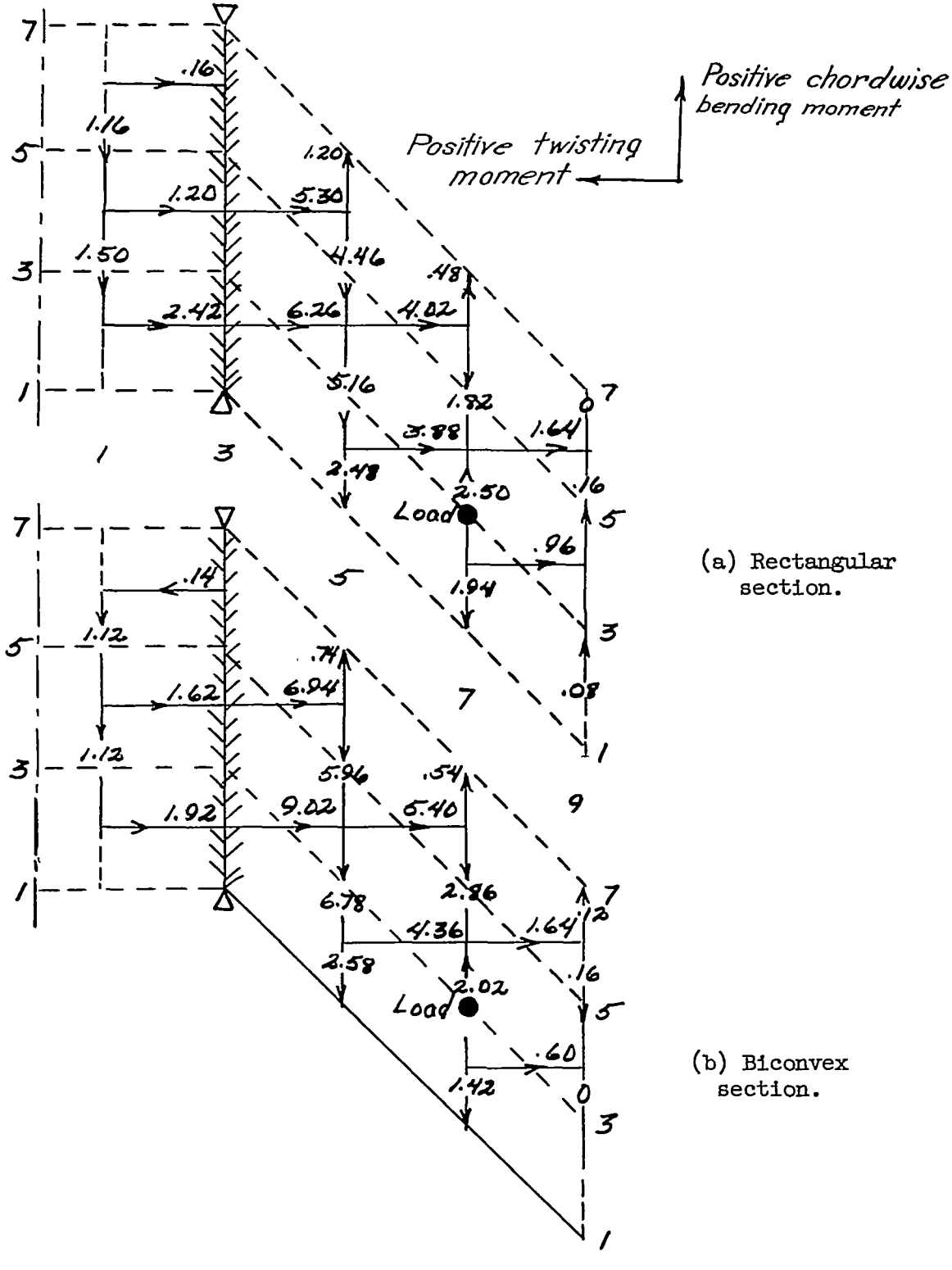

Figure 22.- Distribution of chordwise bending moments and spanwise twisting moments. Load at point 73.

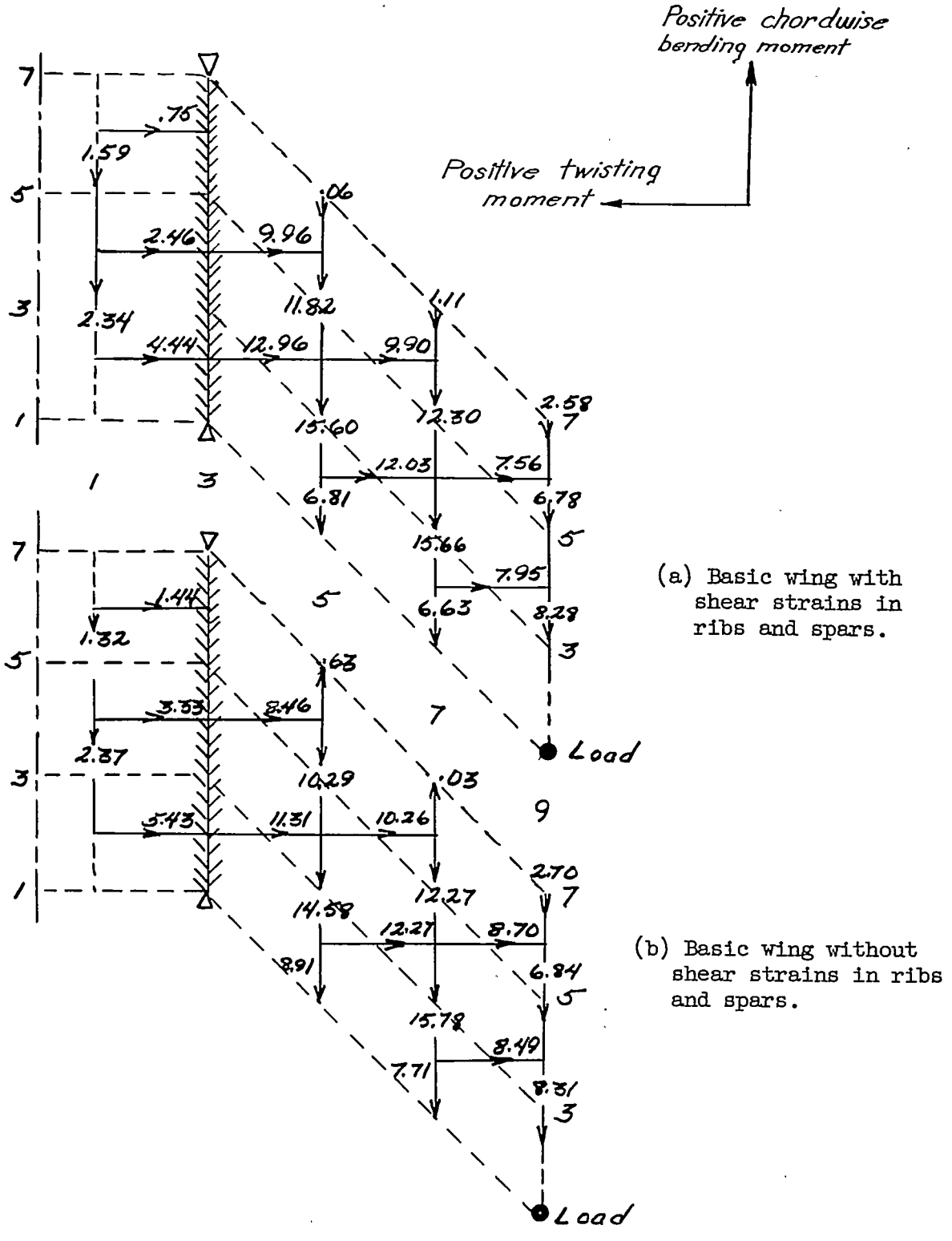

(a) Basic wing with shear strains in ribs and spars.

(b) Basic wing without shear strains in ribs and spars.

Figure 23.- Distribution of chordwise bending moments and spanwise twisting moments. Rectangular section; load at point 91.

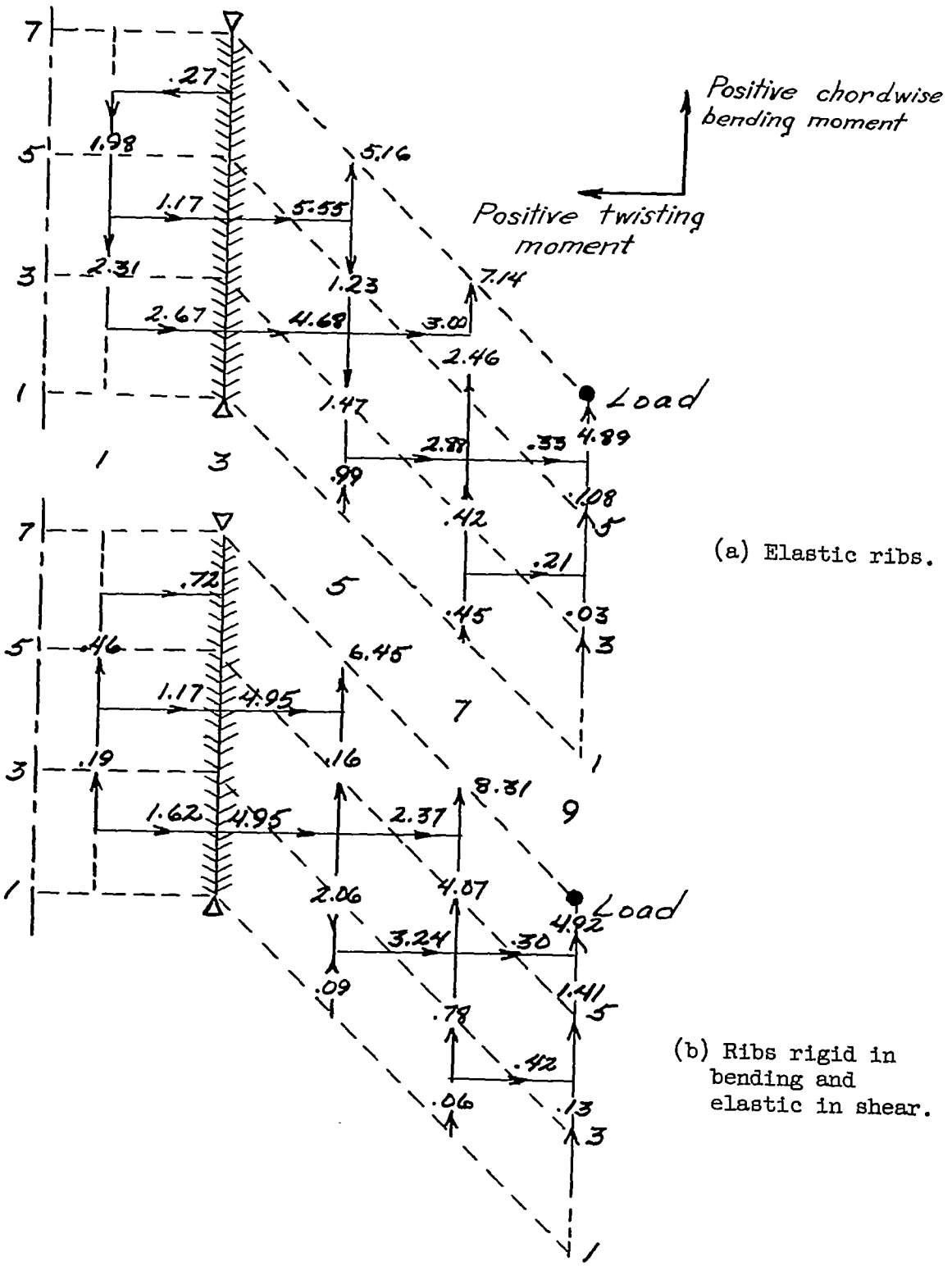

(a) Elastic ribs.

(b) Ribs rigid in bending and elastic in shear.

Figure 24.- Distribution of chordwise bending moments and spanwise twisting moments. Rectangular section; load at point 97.

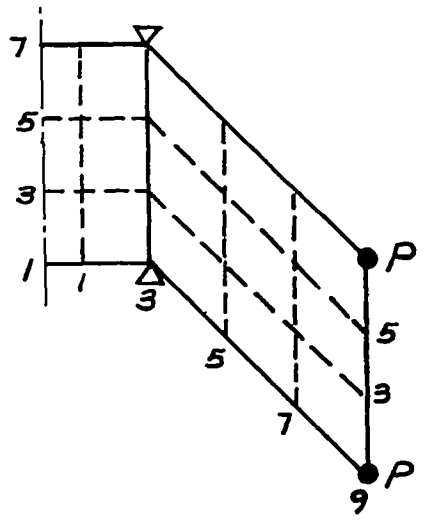

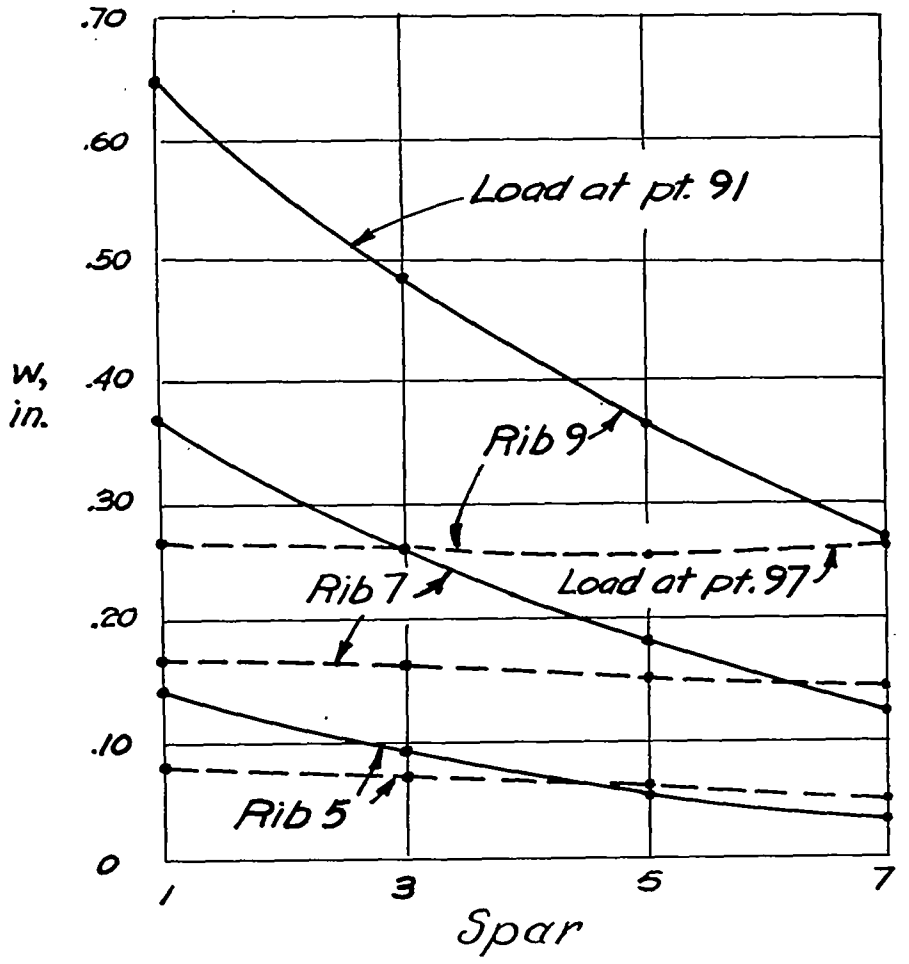

Figure 25.- Chordwise deflections. Biconvex section; P = 1 kip.

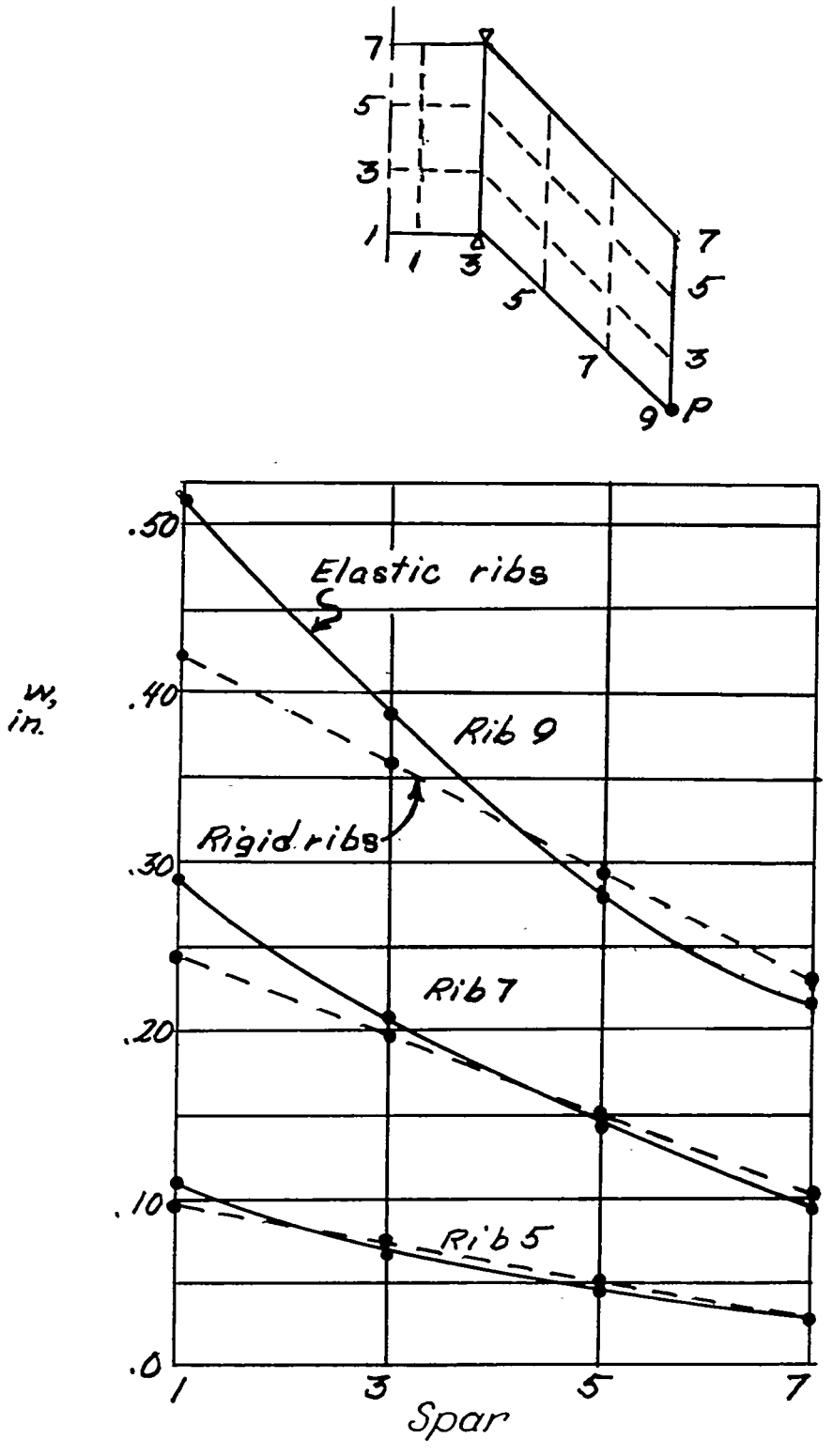

Figure 26.- Chordwise deflections. Rectangular section; load at point 91; P = 1 kip.

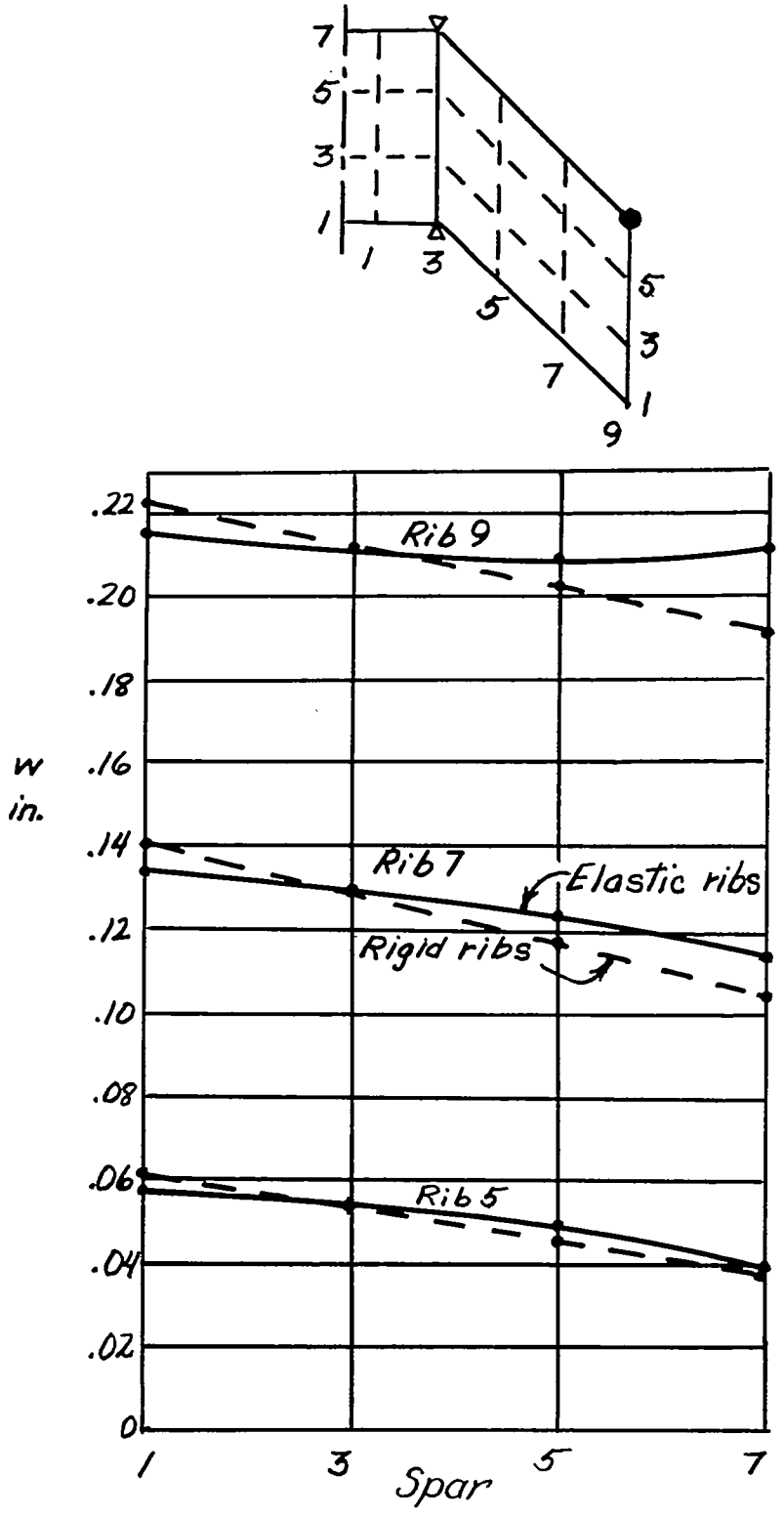

Figure 27.- Chordwise deflections. Rectangular section; load at point 97; P = 1 kip.

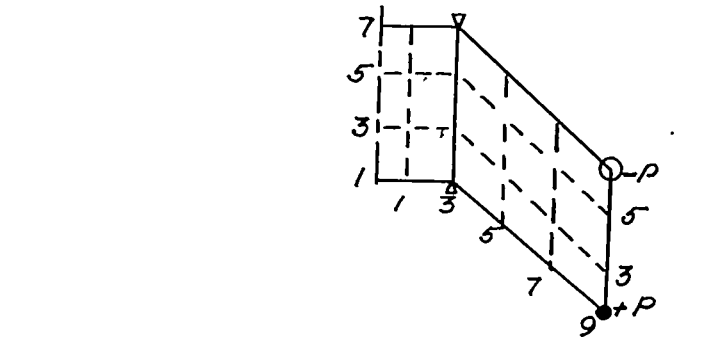

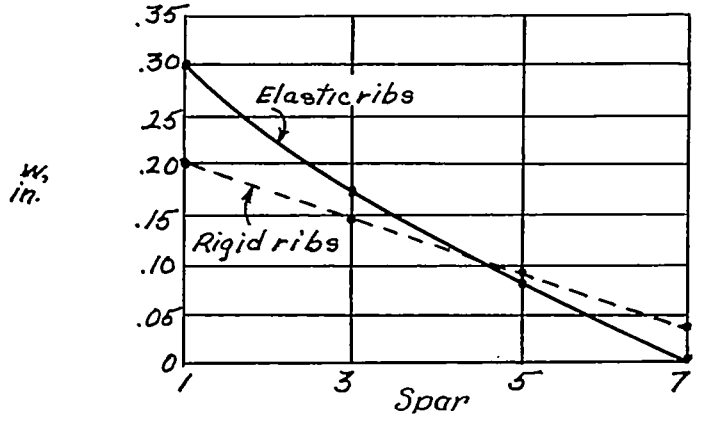

(a) Rib 9.

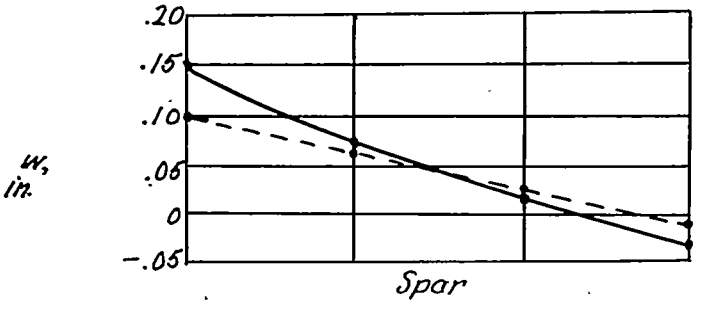

(b) Rib 7.

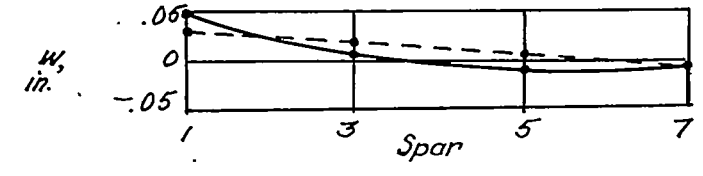

(c) Rib 5.

Figure 28.- Chordwise deflections. Rectangular section; couple applied to tip; P = 1 kip.

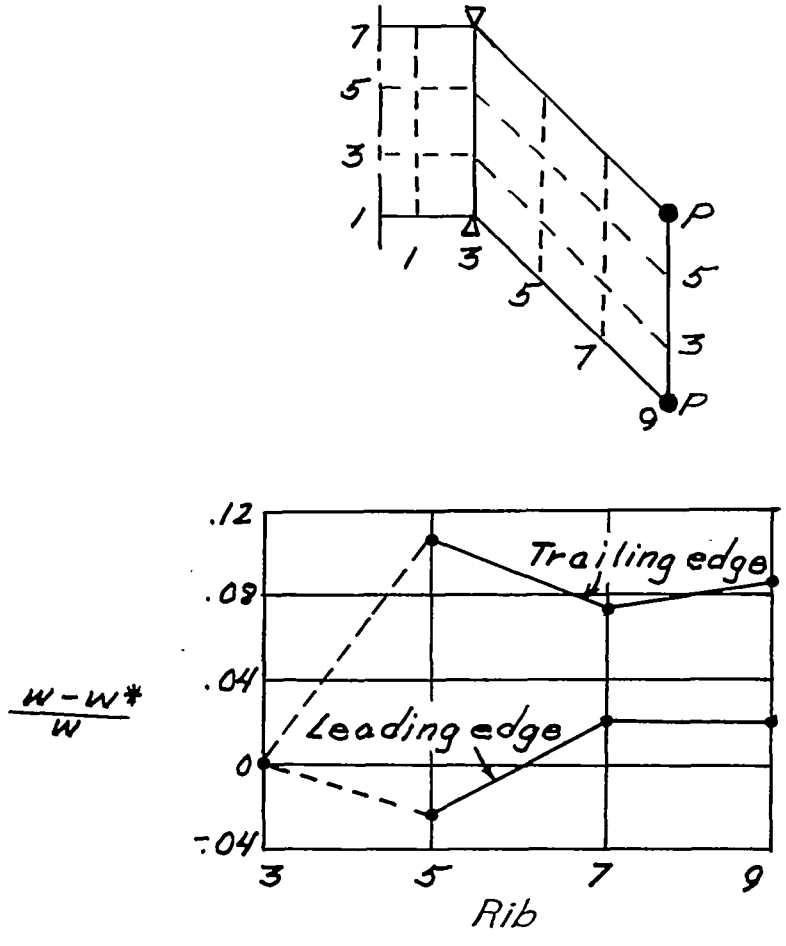

(a) Load at point 91.

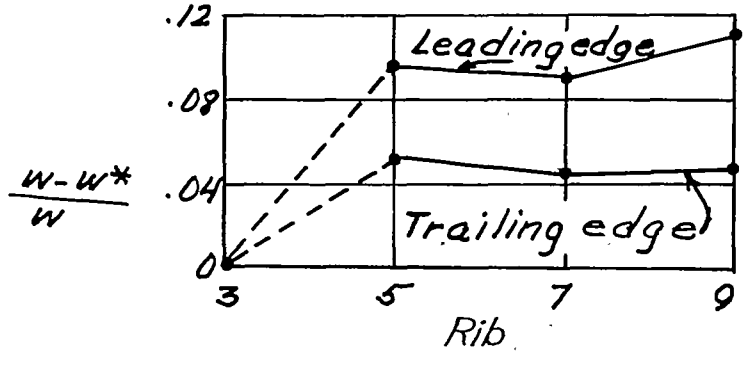

(b) Load at point 97.

Figure 29.- Effect of shear strain in ribs and spars on deflections. Rectangular section; P = 1 kip. w, deflection with shear strain in ribs and spars; w*, deflection without shear strain in ribs or spars.

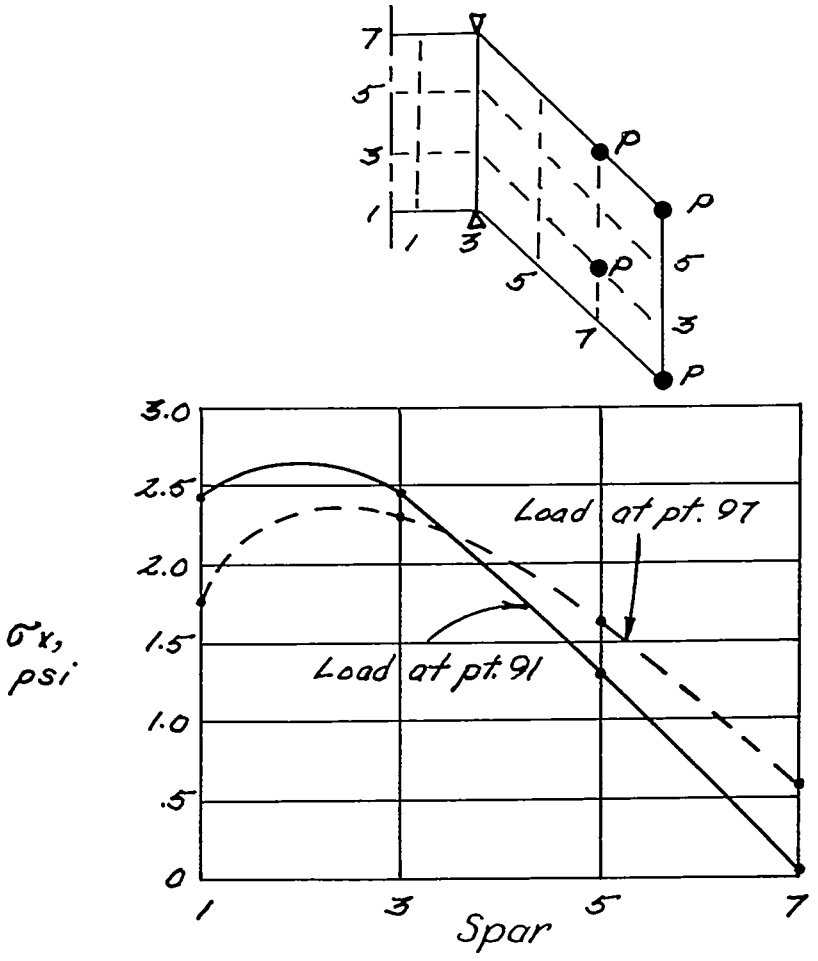

(a) Load at points 91 and 97.

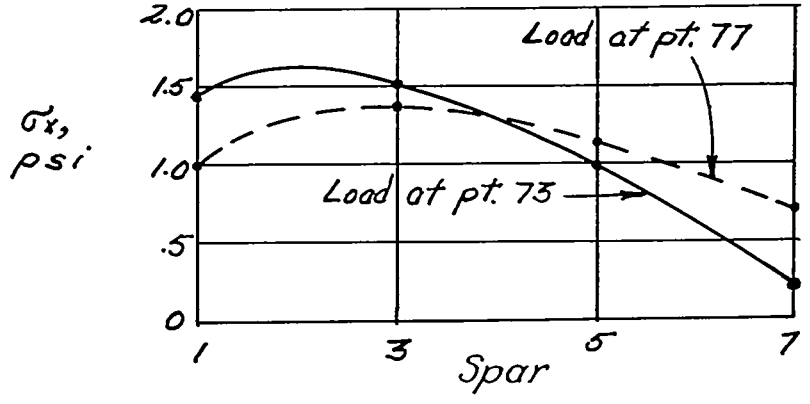

(b) Load at points 73 and 77.

Figure 30.- Chordwise distribution of spanwise normal stress along rib 3. Biconvex section; P = 1 pound.

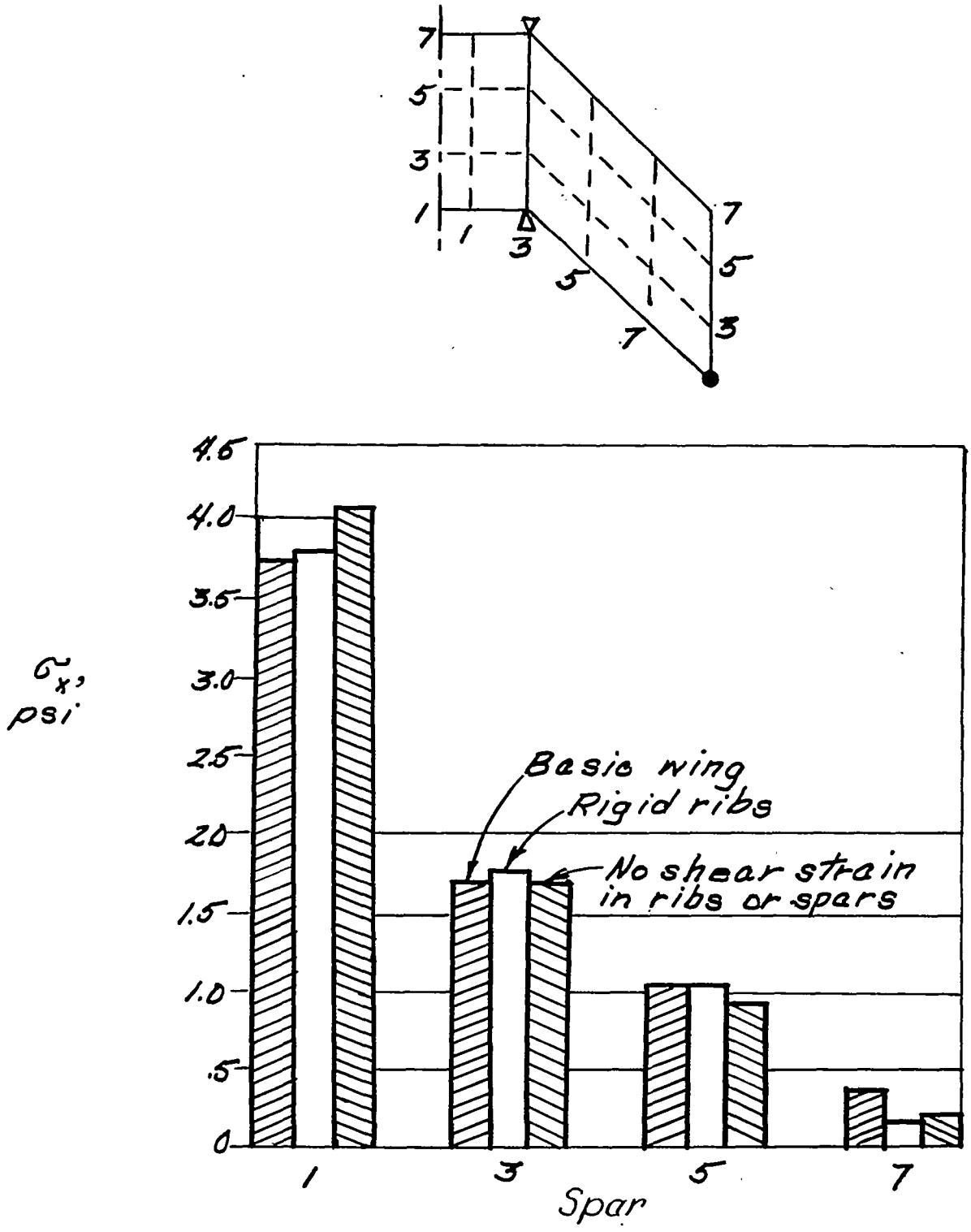

Figure 31.- Chordwise distribution of spanwise normal stress along rib 3. Rectangular section; load at point 91; P = 1 pound.

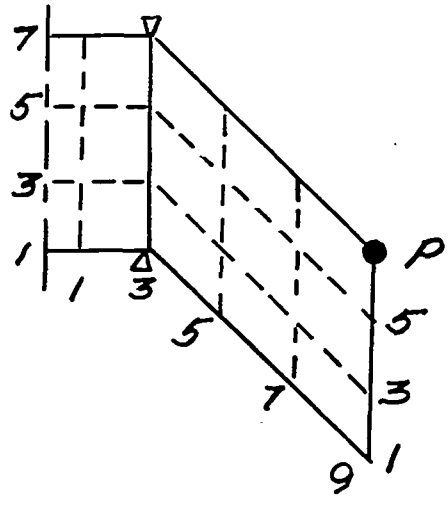

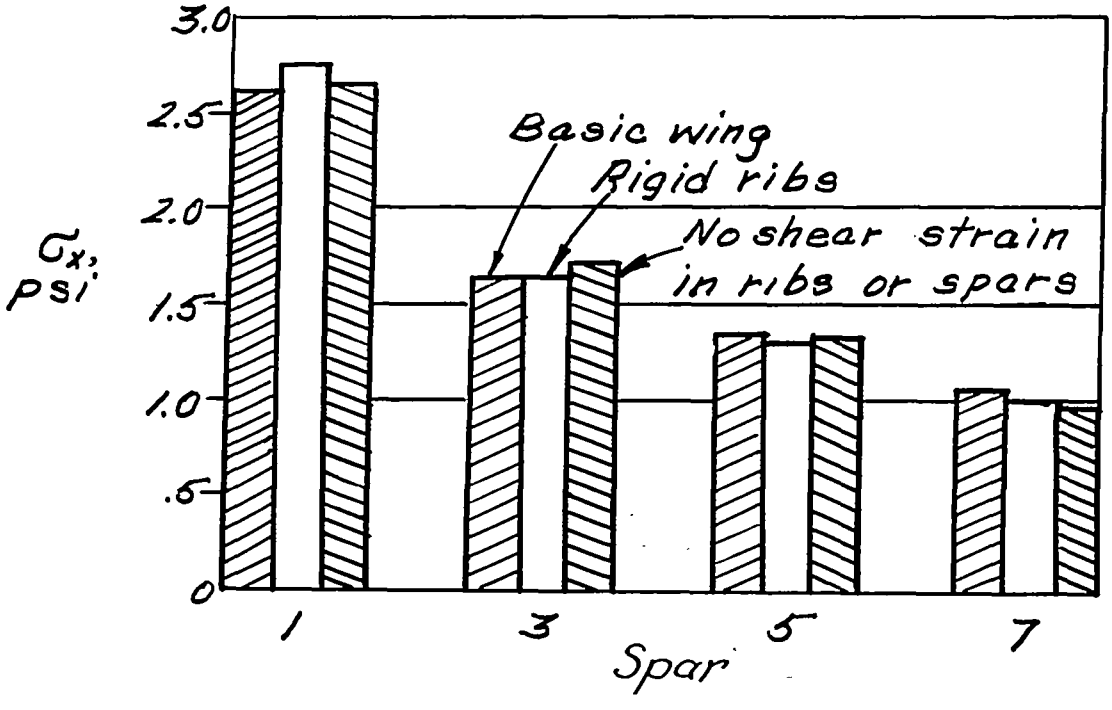

Figure 32.- Chordwise distribution of spanwise normal stress along rib 3. Rectangular section; load at point 97; P = 1 pound.

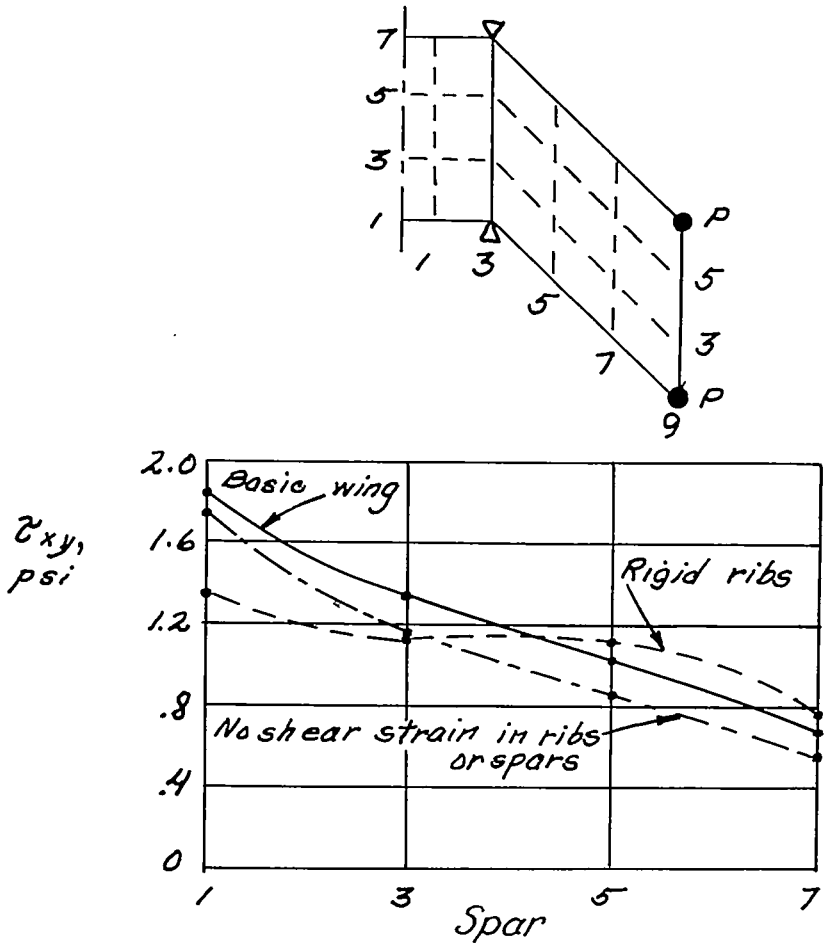

(a) Load at point 91.

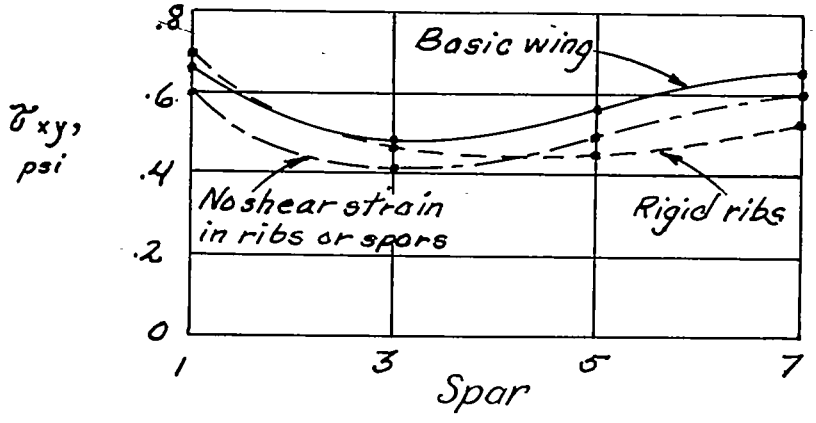

(b) Load at point 97.

Figure 33.- Chordwise distribution of shear stress in skin on section midway between ribs 3 and 5. Rectangular section; load at points 91 and 97; P = 1 pound.

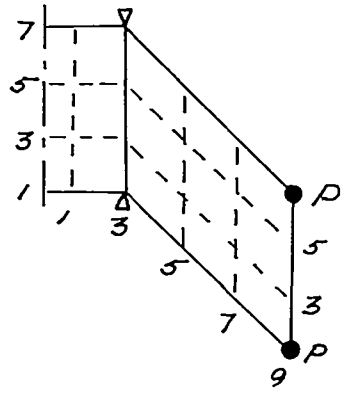

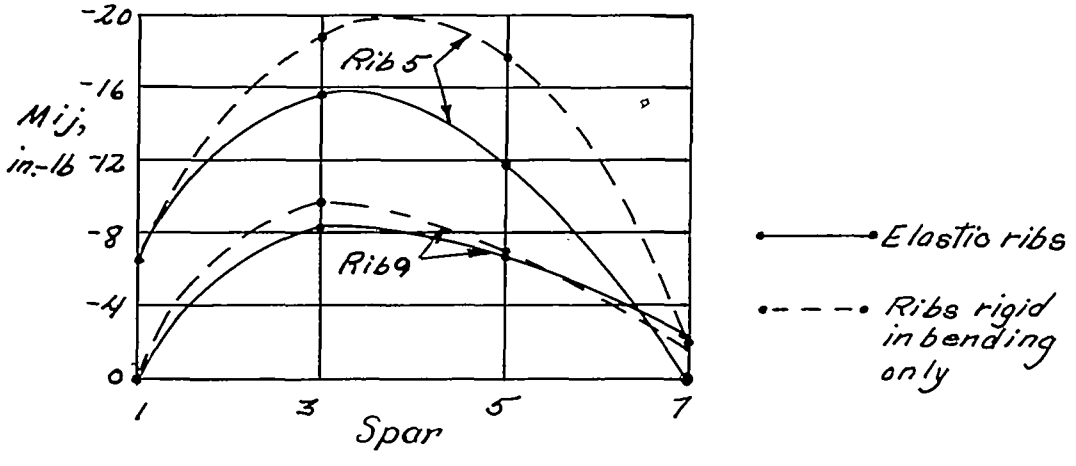

(a) Load at point 91.

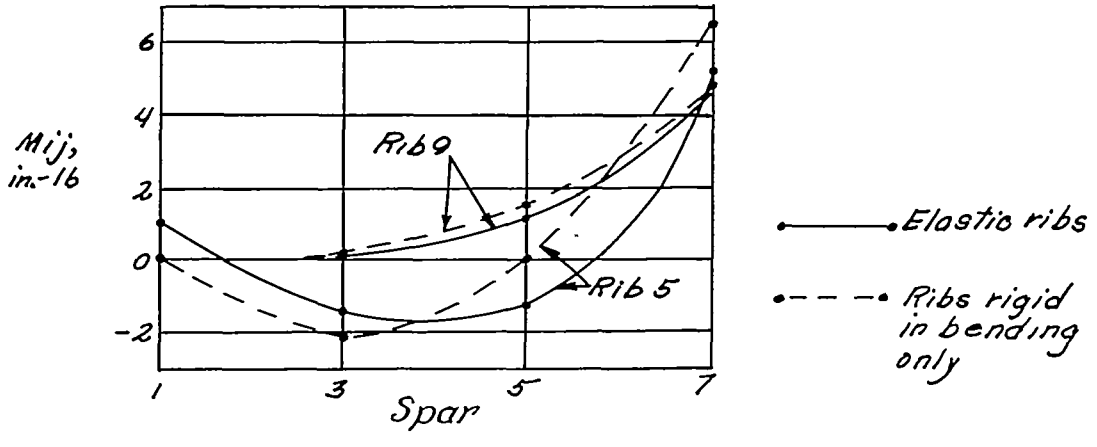

(b) Load at point 97.

Figure 34.- Chordwise bending moments. Rectangular section; P = 1 pound.

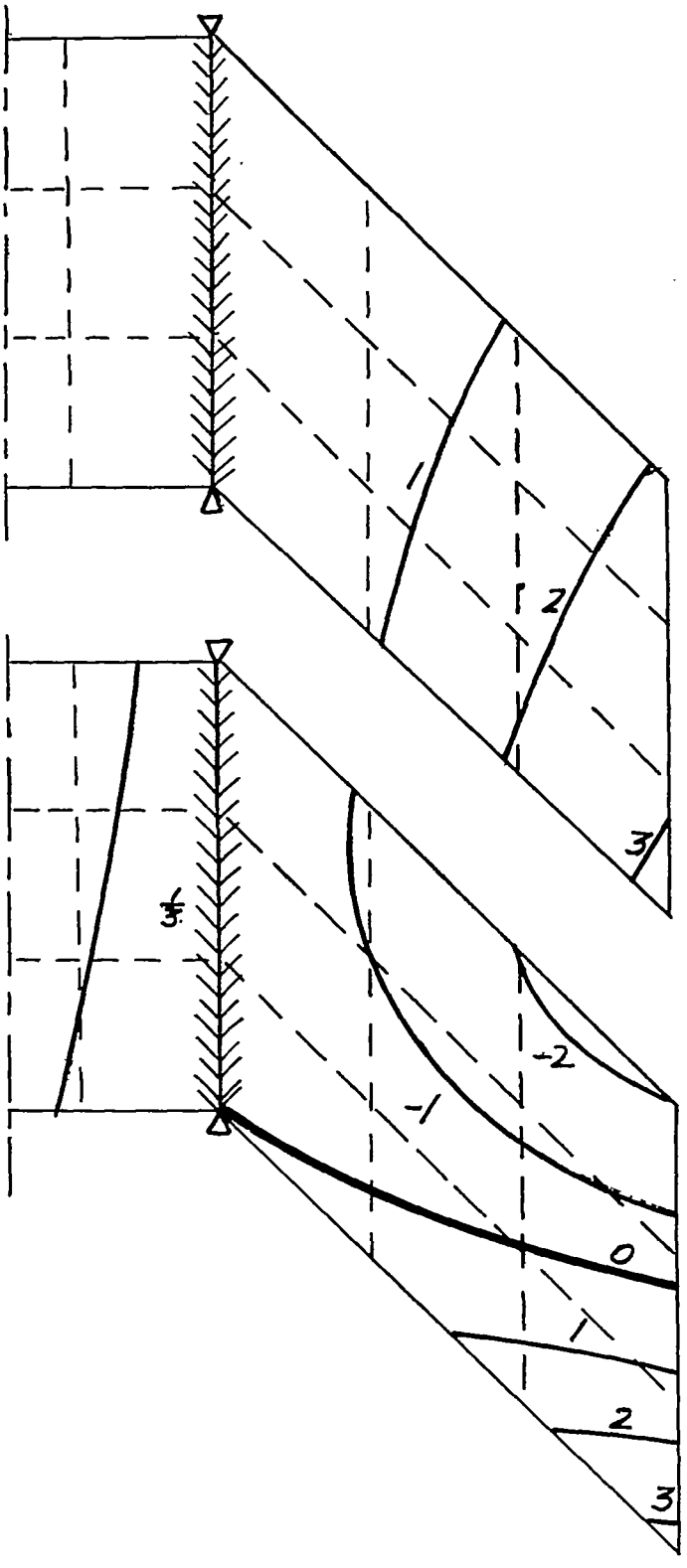

(a) First mode; frequency, 36.0 cycles per second.

(b) Second mode; frequency, 114 cycles per second.

Figure 35.- Symmetric vibration modes. Rectangular section.

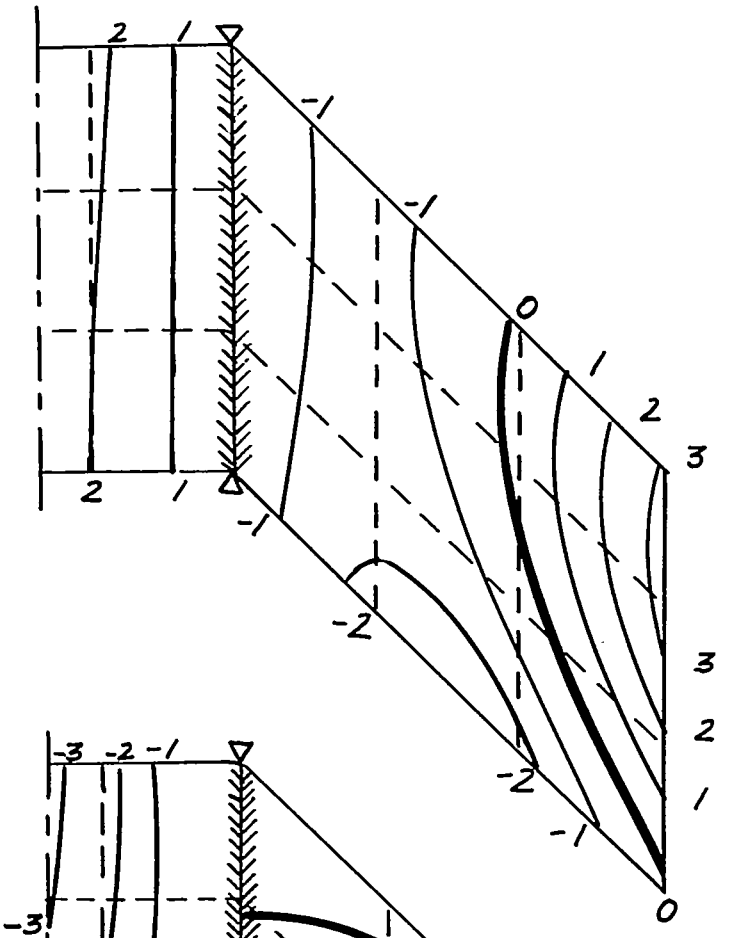

(c) Third mode; frequency, 228 cycles per second.

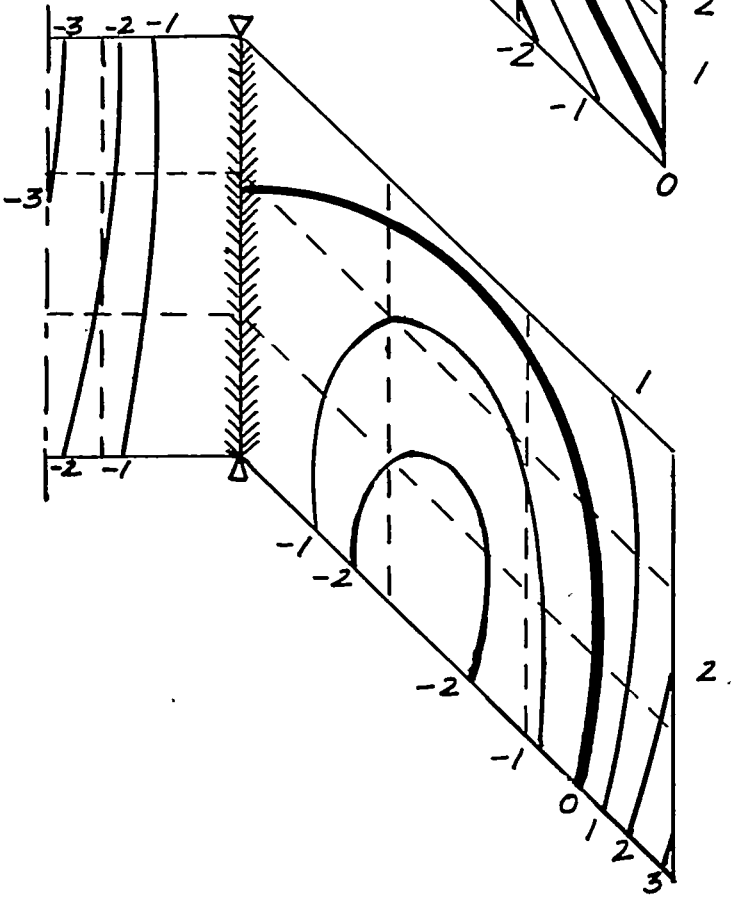

(d) Fourth mode; frequency, 252 cycles per second.

Figure 35.- Concluded.

NACA-Langley - 1-26-54 - 1000